JOURNAL OF GEOPHYSICAL RESEARCH, VOL. 105, NO. D9, PAGES 11,641–11,658, MAY 16, 2000

Revision of the stratospheric bomb $^{14}CO_2$ inventory

Vago Hesshaimer and Ingeborg Levin

Institut für Umweltphysik, University of Heidelberg, Heidelberg, Germany

Abstract. About 4900 values of $^{14}CO_2$ activity have been measured on stratospheric air samples collected between 1953 and 1975 when the major nuclear weapon tests injected large amounts of ^{14}C into the atmosphere. However, the validity of these data published in Health and Safety Laboratory reports was repeatedly criticized and their relevance is thus usually denied in model studies tracing the global carbon cycle with bomb $^{14}CO_2$. To oppose this criticism, we perform here a comprehensive analysis of the measurements and calculate stratospheric bomb $^{14}CO_2$ inventories for the period in question. We find out that the recognized weaknesses of the survey do not justify a general discrimination against the $^{14}CO_2$ observations. Our $^{14}CO_2$ inventories determined using numerical methods to interpolate the observations widely confirm the more "hand-made" results from a former study by *Telegadas* [1971] except in the northern poleward stratosphere. We are also able to clear away the reasons commonly advanced to call into question the stratospheric bomb $^{14}CO_2$ inventories by up to 20%. These findings rehabilitate the most extensive data set of stratospheric $^{14}CO_2$ observations and establish them, together with our corresponding bomb $^{14}CO_2$ inventories, as a valuable observational constraint which should be seriously accounted for in global carbon cycle models and in other studies relying on an accurate simulation of air mass transport in the atmosphere.

1. Introduction

Fortunately, the radiocarbon method developed early enough [*Libby et al.*, 1949] to detect that nuclear weapon tests in the atmosphere perturb natural ^{14}C levels by producing much of so-called bomb ^{14}C. Measurements of the $^{14}CO_2$ activity of stratospheric air (most ^{14}C resides in the atmosphere as $^{14}CO_2$) were included in the global survey STARDUST supported by the United States between 1953 and 1969. The bulk of $^{14}CO_2$ activity values measured during that survey was summarized to determine the time variation of the bomb $^{14}CO_2$ burden in the stratosphere [*Telegadas*, 1971]. In that paper, *Telegadas* [1971, p. 3] proposed to further use the presented distribution of $^{14}CO_2$ "...as a tracer for atmospheric motions and for estimating the exchange rate of CO_2 between the atmosphere and the ocean and biosphere." Indeed, his results were investigated in several studies about air mass motion using two- and three-dimensional models [*Johnston*, 1989; *Shia et al.*, 1993; *Kinnison et al.*, 1994; *Rasch et al.*, 1994]. Strangely enough, the only study budgeting $^{14}CO_2$ in the global carbon cycle which consistently accounted for the stratospheric inventory compiled by Telegadas was by *Hesshaimer et al.* [1994]. All other model studies trying to globally match bomb $^{14}CO_2$ levels observed in the carbon cycle reservoirs [e.g., *Enting et al.*, 1993; *Broecker and Peng*, 1994; *Lassey et al.*, 1996; *Jain et al.*, 1997] solved inconsistencies in their budgets by mistrusting the stratospheric inventories. Justification of this discrimination was already given by *Telegadas* [1971] himself: due to unidentified reasons, the $^{14}CO_2$ activity of samples collected in the lower troposphere aboard aircraft seems to be systematically higher by $\Delta^{14}C \approx 50$-200‰ (for Δ-notation see section 2.1) than observed at comparable ground level stations. A second shortcoming of the data interpretation resides in the fact that Telegadas used hand-made drawings to determine, in an undocumented manner, his stratospheric inventories from the original $^{14}CO_2$ observations. A third often mentioned criticism is that the survey was not intense enough to allow a reliable quantification of the stratospheric bomb $^{14}CO_2$ burden during such a period of intense nuclear tests [*Tans*, 1981; *Broecker et al.*, 1995]. In the present paper we confront ourselves to all these shortcomings and reprocess the data in a way suitable for further investigations. In the following second section we present the entire set of data with enough detail to compute, in the third section, a stratospheric bomb $^{14}CO_2$ burden to be compared with the inventories of Telegadas. In the fourth section, conclusions are drawn from the comparison between the $^{14}CO_2$ activity values published in the Health and Safety Laboratory (HASL) reports and observations from other sources.

Paper number 1999JD901134.
0148-0227/00/1999JD901134$09.00

2. Stratospheric Observations Published in the HASL Reports

The Health and Safety Laboratory reports with numbers 159, 166, 174, 214, and 242 [*Hagemann et al.*, 1965, 1966, 1967, 1969, 1971] present tables containing values of $^{14}CO_2$ activity, along with auxiliary $\delta^{13}C$, $\delta^{18}O$ values, and CO_2 mixing ratios, from whole air samples collected in the project STARDUST between mid-1953 and mid-1969 which are numbered 1 to 6492. Recently, these data also became available on the World Wide Web at the Carbon Dioxide Information Analysis Center (CDIAC) [*Leifer and Chan*, 1998]. About 140 further stratospheric $^{14}CO_2$ activity data from the period mid-1968 to mid-1974 are reported in the HASL reports 246 [*Telegadas et al.*, 1972], 284 [*Sowl et al.*,

1974], and 294 [*Sowl et al.*, 1975]. In the following we refer to the sum of all these reports as the HASL reports, to the sum of the corresponding observations as the HASL observations, and so forth. About 75% of the activity values in the HASL reports were measured on 12 m^3 STP air samples compressed aboard aircraft into nickel-plated spherical steel bottles [*Hagemann et al.*, 1965]. Of the remaining 25%, all $^{14}CO_2$ activities except those in HASL reports 246, 284, and 294 were measured from about 50 m^3 STP air samples transferred after balloon flights from an armored vessel into high-pressure cylinders [*Hagemann and Gray*, 1959]. The activities presented in HASL reports 246, 284, and 294 were measured on samples collected with a molecular sieve technique [*Ashenfelter et al.*, 1972].

Most of the observations from project STARDUST made available as CDIAC database were not initially available on computer systems and had to be retrieved from publications [*Leifer and Chan*, 1998]. As we had already transferred, independently, the same tables from the HASL reports to our computer system, we could identify some 50 misreading errors in the CDIAC database by cross comparison with the results of our computerization. These errors will be reported to the CDIAC.

2.1. Activity Unit Conversions

The $^{14}CO_2$ activities presented in the HASL reports are listed in units of disintegration per minute per gram of carbon (dpm/g C) before and in units of 10^5 atoms of ^{14}C per gram of air (10^5 atoms/g air) after a correction explained by *Hagemann et al.* [1965] for isotopic fractionation and contamination during sample treatment. In all HASL reports except 294 the conversion from corrected activities expressed in dpm/g C to corrected activities expressed in 10^5 atoms/g air is obtained by multiplication with 5.64. The excess $^{14}CO_2$ activities attributable to nuclear weapon tests are obtained by subtracting a prenuclear background activity of 74×10^5 atoms/g air from the corrected activities. Note that we refer to this definition when using synonymously "bomb inventory" or "excess inventory" although assuming a constant prenuclear background neglects the natural variability of $^{14}CO_2$ activities in the atmosphere. Also bear in mind that about 5×10^5 atoms ^{14}C/g air of the stratospheric activity excess over tropospheric values result not from bomb input but from the altitude distribution of ^{14}C production by cosmic ray neutrons [*Lingenfelter*, 1963; *O'Brien et al.*, 1991]. The following equation allows to convert from corrected excess activities $A_{1E5\ \mathrm{atoms/g\ air}}$ expressed in units of 10^5 ^{14}C atoms per gram of air to corrected activities $A_{\mathrm{dpm/g\ C}}$ expressed in units of dpm/g C:

$$A_{\mathrm{dpm/g\ C}} = \frac{A_{1E5\mathrm{atoms/g\ air}} + 74}{5.64} \quad . \qquad (1)$$

The values of 5.64 and of 74 are based on an atmospheric CO_2 mixing ratio of 313 ppm (assumed to be constant), on the relative molecular mass of carbon (12.01) and of air (28.96), on the half-life of ^{14}C (5730 years) and on a specific activity of 13.1 dpm/g C for the "atmospheric prenuclear background in the early 1950s." Note that *Telegadas* [1971] and *Telegadas et al.* [1972] refer to 13.17 ± 0.04 dpm/g C as being 0.95 of the National Bureau of Standards (NBS) oxalic acid standard activity measured at the Argonne National Laboratory (ANL). For the present investigation we assume that their measurement of 13.17 dpm/g C was correct and lower than the modern value of 13.56 ± 0.07 dpm/g C measured for 0.95 of the NBS oxalic acid standard corrected for decay and fractionation [*Karlén et al.*, 1968; *Olsson*, 1970; *Stuiver and Polach*, 1977] due to the absence of correction for $\delta^{13}C$ fractionation and for ^{14}C decay in their laboratory. If, however, it comes out that our assumption is wrong and that the absolute activity measurements at ANL was too low by β = 13.17/13.56, then all HASL activities and all corresponding activities in the present paper must be multiplied with $1/\beta$ = 1.03. We use the following equation to convert from HASL activities $A_{\mathrm{dpm/g\ C}}$ expressed in dpm/g C to $\Delta^{14}C$ expressed in per mil (‰):

$$\Delta^{14}C\ (‰) = \frac{A_{\mathrm{dpm/g\ C}}}{13.56}\left(1-2\left(\frac{25-7.1}{1000}\right)\right)1000-1000\,, \qquad (2)$$

assuming the same constant value of –7.1‰ for atmospheric $\delta^{13}CO_2$ [*Hagemann et al.*, 1965] as in the HASL reports. For the sake of simplicity we use the same constant factor of 5.64 to convert from activities in dpm/g C to activities in 10^5 atoms/g air in all our figures except Figure 7. However, we provide in Tables 1 and 2 the parameters D and f allowing to correct this conversion factor taking into consideration long-term variations of the CO_2 mixing ratio. Finally, note that in HASL report 294, *Sowl et al.* [1975] used a multiplication factor of 5.95, corresponding to an atmospheric CO_2 mixing

Table 1. Properties of Our Stratospheric Subdivisions for Which Mean $^{14}CO_2$ Activities Are Listed in Table 2

Stratospheric Subdivision		D	Air Mass, 10^{15} kg
Northern Hemisphere			
Poleward	High	----	12
	Upper	-2.5	46
	Middle	-1.9	96
	Lower	-2.7	243
Equatorward	High	----	12
	Upper	-1.5	46
	Lower	-0.5	96
Southern Hemisphere			
Equatorward	High	----	12
	Upper	-1.3	46
	Lower	-0.2	96
Poleward	High	----	12
	Upper	-2.2	46
	Middle	-0.7	96
	Lower	-0.2	243

The parameter D completes the parameter f in Table 2 and approximates the difference expressed in ppm between the yearly mean CO_2 mixing ratio in a particular stratospheric subdivision and the yearly mean CO_2 mixing ratio observed at Mauna Loa station [*Keeling and Whorf*, 1990]. The values for D are best estimates for 1965 as calculated from stratospheric CO_2 mixing ratios predicted by a carbon cycle model [*Hesshaimer*, 1997] optimally matching the mean $^{14}CO_2$ activities of *Telegadas* [1971] up to 30 km height. Bear in mind that D does not account for the seasonal variation of CO_2 mixing ratio in the stratosphere which can have a mean peak-to-peak amplitude of up to 4 ppm in the northern lower poleward subdivision according to our carbon cycle model. Air masses for the different stratospheric subdivisions were calculated according to the U.S. Standard Atmosphere (1976). The air masses of all stratospheric subdivisions sum up to a total of 1.102×10^{18} kg which corresponds to 21.5% of the total dry air mass of the Earth atmosphere [*Trenberth and Guillemot*, 1994].

ratio of 330 ppm, but we rescaled these results by multiplication with 5.64/5.95 to remain consistent with the other HASL reports.

To avoid confusion, note that we will always refer to activities expressed in the "absolute" scale, not in the "Δ" or in the "excess ^{14}C" scale, when comparing activities without particular specification of the unit. For example, if we write that a sample activity is lower by 10% than another activity and if the other activity is 28.1 dpm/g C = 84.5×10^5 excess ^{14}C atoms per gram of air or $\Delta^{14}C \approx 1000‰$, it means that the value of the sample activity is $28.1\times0.9 = 25.3$ dpm/g C which corresponds to a depletion by about 20% of the sample activity value expressed either in excess ^{14}C units (68.6×10^5 excess ^{14}C atoms per gram of air) or in $\Delta^{14}C$ units (800‰).

2.2. Extent of the Survey

Nearly all northern hemispheric air samples from the HASL reports were collected over the American continent and over the Atlantic and Pacific Oceans. Some sampling took place in the region of Singapore aboard United Kingdom aircraft. In the Southern Hemisphere the samples were collected over the American and Australian continents and their adjacent waters. The HASL tables report the mean latitude, altitude and date of each sample collection but not its mean longitude. Several distinguishing features prevent this lacuna from being a major weakness of the HASL survey. In the Northern Hemisphere most of the samples were collected over North America and the Pacific Ocean. These locations are longitudinally on the opposite side of the world with respect to the locations of nuclear weapon tests by the former Soviet Union which injected about half of the total bomb ^{14}C into the atmosphere. Therefore at least in the case of Soviet detonations the corresponding $^{14}CO_2$ activity excess observed over the United States and the Pacific Ocean should reflect zonal mean conditions over all longitudes at corresponding heights and latitudes. Furthermore, a comparison between a set of HASL samples collected over the United States between 40°N and 80°N and observations at about 60°N and 7°W to the northwest of the British Isles (Figure 1) reveals a great similitude of activity excursions after strong nuclear detonations which took place at about 60°E over the former Soviet Union. Both the time delay between nuclear detonations and $^{14}CO_2$ activity increases as well as the similar amplitude of corresponding peak activities shown in Figure 1 indicate that the bomb $^{14}CO_2$ input signals were longitudinally homogenized within about 1 month. For the above reasons we consider that quarterly means of the HASL activities represent valid zonal means, and we do not analyze the longitudinal repartitioning of $^{14}CO_2$ activity in our study.

The height versus time representation of sampling locations in Figure 2a shows that above 20 km most HASL samples were collected during balloon flights, whereas below 20 km and after 1960, aircraft sampling was preponderant. In a small region, balloon and aircraft sampling locations overlap well enough between 1962 and 1965 to allow comparison of both sets. The $^{14}CO_2$ activities of single samples collected in this region show a good agreement between balloon and aircraft observations (Figure 3). The height versus latitude representation of sampling locations in Figure 2c reveals that the HASL survey was much denser in the Northern than in the

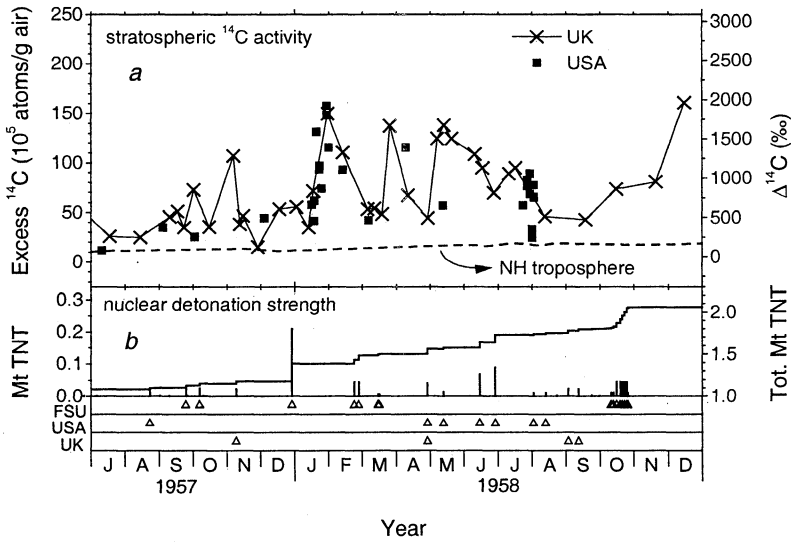

Figure 1. (a) Observations of $^{14}CO_2$ activity in stratospheric air between 10 and 15 km above sea level (asl) from the HASL reports along with (b) reported strengths of nuclear weapon detonations expressed in equivalent megatons (Mt) of TNT [*Rath*, 1988]. Crosses, activity of samples collected until 1959 aboard United Kingdom aircraft to the northwest of the British Isles (approximately 60°N, 7°W). Solid squares, activity of samples collected above the United States. The dashed line in Figure 1a indicates the background $^{14}CO_2$ activity in the northern hemispheric troposphere [*Tans*, 1981]. The activity is expressed in units of 10^5 excess ^{14}C atoms per gram of air on the left-hand side of the figure and in the Δ scale on the right-hand side. Open triangles in Figure 1b indicate which nation was responsible for a given nuclear detonation. In the former Soviet Union (FSU), nuclear bombs were mostly detonated between 50°N and 80°N from 45°E to 80°E. The major British (UK) and American (USA) nuclear tests took place over the Pacific Ocean between 0°N and 20°N from 170°E to 150°W at that time. The solid line in Figure 1b traces the total strength of all bombs detonated worldwide since 1945 (right axis scale).

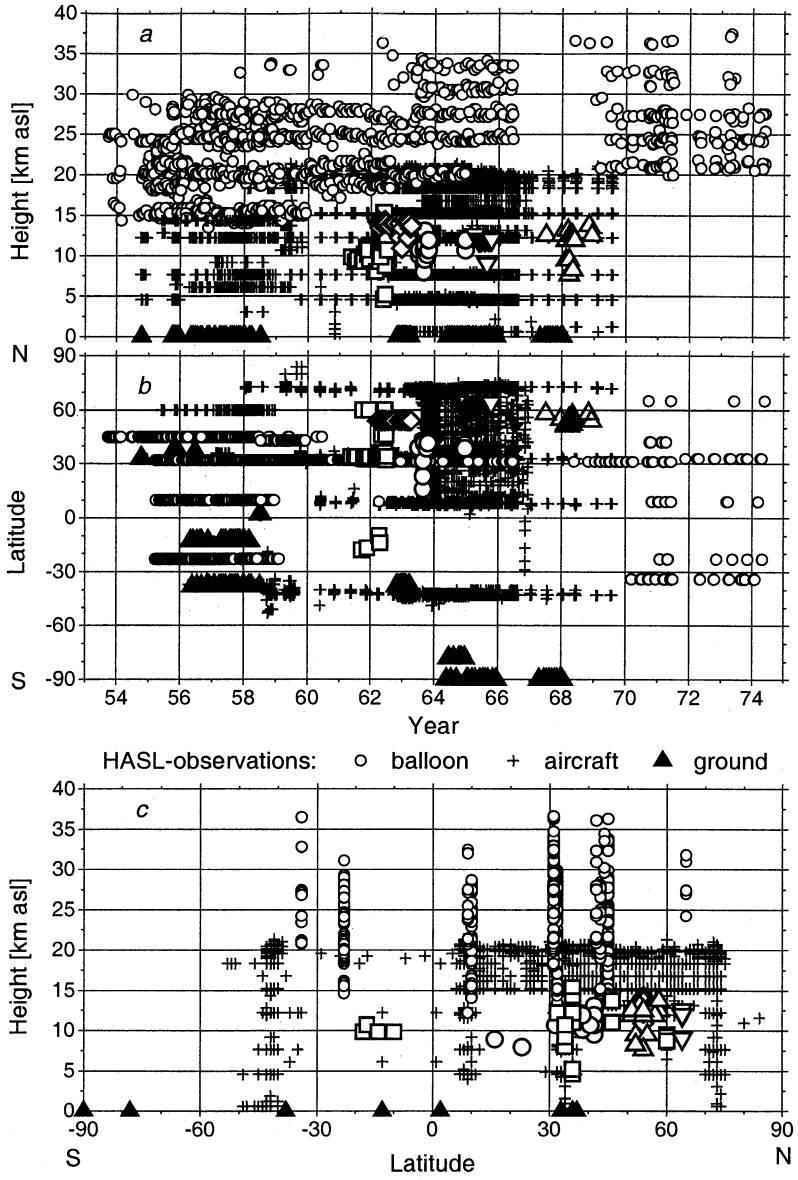

Figure 2. (a) Height versus time, (b) latitude versus time, and (c) height versus latitude representations of $^{14}CO_2$ sampling locations found in the HASL reports and in other publications. In the HASL locations a distinction is made between ground level samples (solid triangles), balloon samples (small open circles), and aircraft samples (pluses). The sampling locations of observations found in other publications are reported using open squares [*Fergusson*, 1963], open diamonds [*Godwin and Willis*, 1964], large open circles [*Berger et al.*, 1965], open down triangles [*Nydal and Lövseth*, 1983] and open up triangles [*Walton et al.*, 1970]. The samples of Fergusson and of Berger et al. were collected over the continental United States and the Caribbean, those of Nydal and Lövseth were collected over Norway, and those of Godwin and Willis and of Walton et al. were collected in the vicinity of the British Isles.

Southern Hemisphere with a particularly high sampling density between 5°N and 75°N at altitudes ranging from 15 to 22 km. In the Southern Hemisphere the sampling density is high only near 40°S. Also note that balloon sampling in the stratosphere up to 30 km or higher was concentrated near six singular latitudes. However, Figure 2b shows that only the balloon profiles sampled near 30°N cover almost continuously the time range between 1955 and 1972. Furthermore, Figure 2b reveals that the period with particularly dense atmospheric sampling in the Northern Hemisphere ranges only from mid-1963 to early 1967 and that the latitudinal sampling was relatively sparse in 1960 and 1961.

3. Determination of the Stratospheric Bomb ^{14}C Inventories

Telegadas [1971] summarized the $^{14}CO_2$ data between 1955 and 1969 published in the HASL reports by judiciously subdividing the stratosphere up to 30 km of each hemisphere into four compartments (Figure 4) for which he determined the time variation of the bomb $^{14}CO_2$ burden. To determine his inventories, Telegadas subdivided the year into four quarterly intervals (December–February, March–May, June–August, and September–November), inserted all HASL observations sampled during a quarterly interval into a height versus lati-

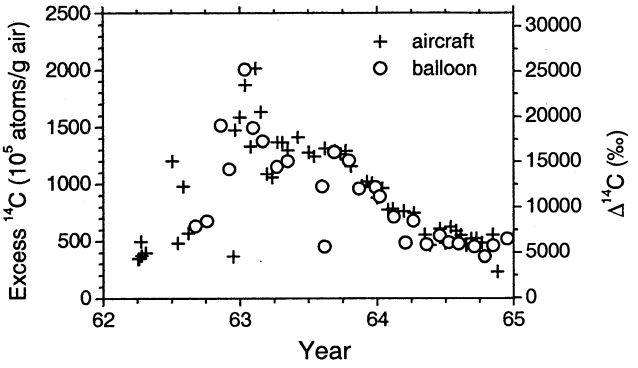

Figure 3. The $^{14}CO_2$ observations from balloon samples (open circles) are compared with activities of samples collected aboard aircraft (pluses). The comparison is restricted to a small region ranging from 30°N to 35°N and from 19.5 to 20.5 km asl where balloon and aircraft HASL data overlap. The activity is expressed in units of 10^5 excess ^{14}C atoms per gram of air on the left-hand side of the figure and in the Δ scale on the right-hand side.

tude representation of the atmosphere, drew hand-made contour lines to interpolate the observed $^{14}CO_2$ activities, and finally integrated the interpolated activities over each of his stratospheric subdivisions. Corresponding mean $^{14}CO_2$ activities can be obtained after division of these inventories by the air mass of each compartment as specified by *Telegadas* [1971].

3.1. New Calculation and Comparison With Telegadas

Here we apply the procedure of *Telegadas* [1971] to the entire HASL data set using exclusively numerical methods. After collection of the data into quarterly diagrams subdivided like those of Telegadas we use a Delaunay triangle-based linear interpolation [*Fortune*, 1987] to determine the activities inside the convex hull of all quarterly sampling locations (see Figure 5a). We refer to section 3.2.2 for details on our Delaunay triangulation. To obtain partial $^{14}CO_2$ inventories, the interpolated specific activity is integrated versus air mass over the intersection between each stratospheric subdivision and the convex hull of sampling locations. The integration is based on an adaptive recursive Simpson's rule and uses the barometric formula as prescribed in the U.S. Standard Atmosphere (1976) for the conversion from height to pressure. We finally obtain mean $^{14}CO_2$ activities for each stratospheric subdivision (Figure 6) when dividing its partial inventory by the air mass of its intersection with the convex hull of sampling locations. The corresponding activity values expressed in dpm/g C are listed in Table 2. For each stratospheric subdivision the data coverage is interpreted as a confidence value attributable to the corresponding mean activity (shaded bars in Figure 6) which is obtained from the ratio of the subdivision air mass included in the convex hull of sampling locations divided by the subdivision's total air mass listed in Table 1. For example, a stratospheric subdivision with 100% of data coverage is entirely included in the corresponding quarterly convex hull of sampling locations.

Our results compare well with those from *Telegadas* [1971] except in the middle poleward subdivision of the Northern Hemisphere where our activities are lower by 20% until mid-1962 then by 30-50% until early 1963 and by 10% after (Figure 6). Looking more into the details of the comparison reveals some further noticeable differences. In the northern lower equatorward stratosphere during 1963 our compilation peaks at activities lower by 30%. In the northern upper stratosphere our activities in 1962 rise steeply about half a year earlier mainly due to a sharp peak in the upper equatorward subdivision. In the southern upper stratosphere between mid-1963 and mid-1966 we find values higher by 20% than those of Telegadas. Note that in both hemispheres the smallest observational coverage until 1970 is found in the upper poleward subdivisions. In the Southern Hemisphere the observational coverage is often less than 50%, but this is not critical due to a large dilution there of the mainly northern hemispheric nuclear bomb input signals. In terms of the total stratospheric bomb ^{14}C inventory, Figure 7a shows that the results of what we will call our standard calculation do not differ much from the results of *Telegadas* [1971].

As one example illustrating the accuracy of our standard calculation, let us examine the $^{14}CO_2$ input through a Chinese bomb equivalent to 3 Mt of trinitrotoluene (TNT) detonated at 40°N in June 1967 which is far the strongest nuclear test reported for the years 1965 to 1967 [*Rath*, 1988; *Yang et al.*, 1999] and should produce about 3×10^{26} atoms ^{14}C corresponding to a standard yield of 10^{26} atoms ^{14}C per megaton of

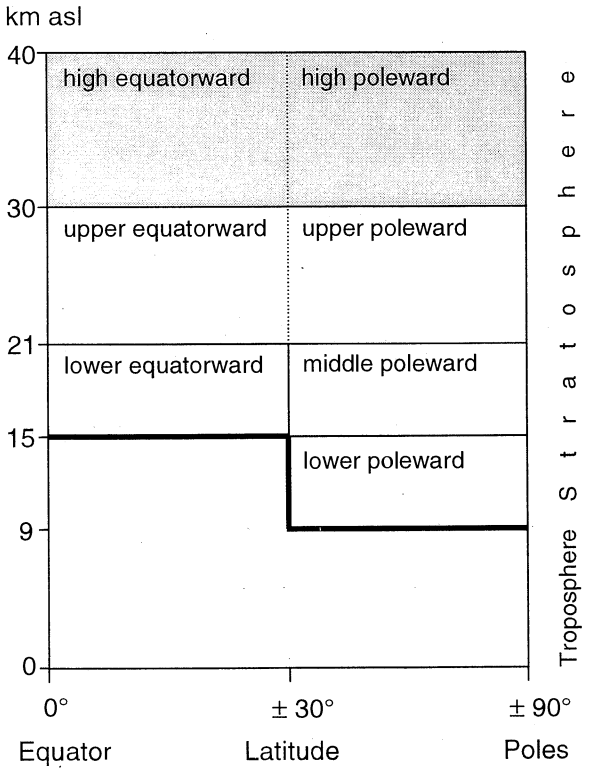

Figure 4. Schematic subdivision of the stratosphere as used by *Telegadas* [1971] in each hemisphere to determine his bomb $^{14}CO_2$ inventories. The dotted line in the upper and high stratosphere and the gray background in the high stratosphere indicate that Telegadas did neither subdivide the upper stratosphere nor account for the high stratosphere as we did. The thick line represents the tropopause. Notice that Telegadas placed his vertical subdivisions at 0, 30, 50, 70, and 100 kilofeet and we approximated these values by 0, 9, 15, 21, and 30 km to determine our inventories. The air mass contained in each of our subdivisions is listed in Table 1.

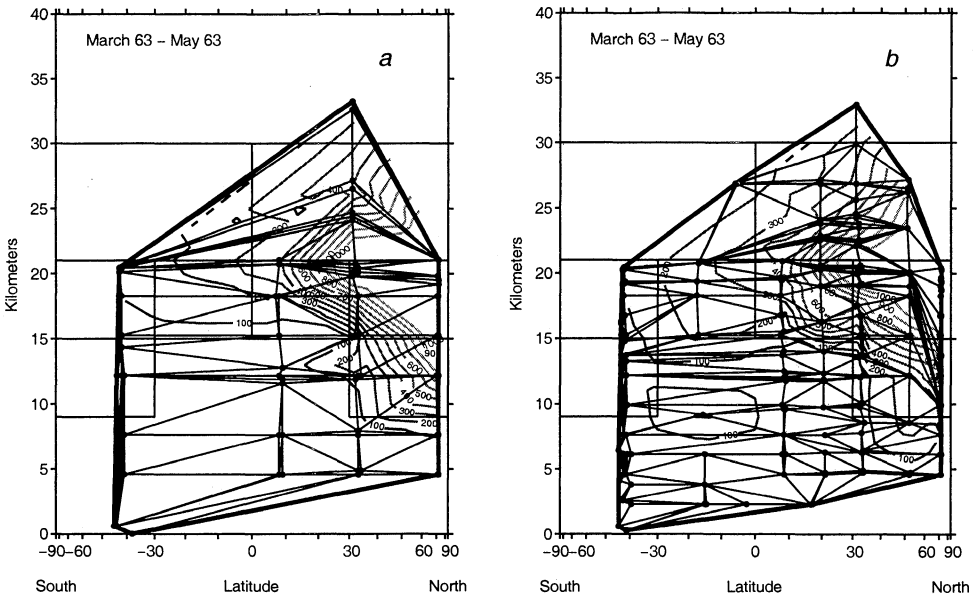

Figure 5. (a) Specimen of a quarterly collection of HASL sampling locations (thick solid circles) obtained for March-May 1963. The thick line represents the convex hull of the quarterly sampling locations. Thin lines connecting the sampling locations represent segments of the Delaunay triangulation on the base of which the $^{14}CO_2$ activities were linearly interpolated to determine $^{14}CO_2$ inventories. Contour lines of the obtained interpolated $^{14}CO_2$ activities up to 1000×10^5 atoms/g air are also put under the figure. For better understanding we did not draw the slight distortion of triangle and hull segments due to the fact that our interpolation procedure took place in a Cartesian latitude-height geometry, whereas a sinusoidal representation of the latitude is used in the figure. Also note that we used the mean activity for locations repeatedly sampled in the quarterly diagrams. (b) Same as Figure 5a except that the contours and triangulation refer to a new set of sampling points based on the original quarterly sampling set shown in Figure 5a. See section 3.2.2 for more explanations.

TNT [*Hesshaimer et al.*, 1994]. *Telegadas* [1971, p. 11] examined the same detonation and concluded that his stratospheric inventories do not reflect this explosion "...probably because the debris had little chance to spread latitudinally into the limited sampling network." In contrast, scrutinizing the results of our standard calculation in Figure 6 reveals an increased $^{14}CO_2$ activity in the lower stratosphere of the Northern Hemisphere which we can estimate in terms of ^{14}C atoms using the results listed in Table 2. For the northern lower equatorward stratosphere the mean activity increase between early 1967 and mid-1967 is 3.25 dpm/g C which corresponds to 1.8×10^{26} atoms ^{14}C in the entire subdivision. In the northern lower poleward stratosphere the seasonal minimum in mid-1967 has been filled up by ^{14}C resulting from the detonation. We compare the activity difference between mid-1966 and early 1967 with the activity difference between mid-1967 and early 1968 and estimate that this filling up corresponds to about 0.5 dpm/g C = 0.7×10^{26} atoms ^{14}C. The sum of $1.8+0.7 = 2.5\times10^{26}$ atoms ^{14}C already represents a reasonable lower limit for the expected total input of 3×10^{26} atoms ^{14}C, although it does not include a corresponding balance for the northern middle poleward stratosphere which cannot be determined in a simple way from the observations. However, for a bomb detonated at 40°N we expect that the ^{14}C inputs to the middle poleward and to the lower equatorward subdivisions are of comparable magnitude and this indicates that the yield of 10^{26} atoms ^{14}C per megaton of TNT is too low if the detonation strength of 3 Mt of TNT is correct.

3.2. Estimation of Errors in the Inventories due to Data Selection and Interpolation

In Figure 6 we report as "percent of data coverage" the portion of air mass contained in the convex hull of sampling locations, although this validity estimator of the mean $^{14}CO_2$ activities can be substantially biased. In the worst case during a given quarterly interval a subdivision could be 100% inside the convex hull of sampling locations without any observational sample in it. This is why we further examine how far two categories of errors reduce the validity of our mean activities based on the HASL survey. In the first category we estimate errors related with data selection in time, space, and activity level, and in the second category we scrutinize interpolation choices of more numerical type like the coordinate system units, the polynomial order or the triangle mesh structure and estimate their impact on the obtained activities.

3.2.1. Errors due to selection. We split up the HASL observations into quarterly intervals to determine mean $^{14}CO_2$ activities in the stratospheric subdivisions. This corresponds to a data selection on the time axis and has the drawback of possibly smoothing down the main activity peaks. In Figure 8 this impact is estimated through comparison between activity curves resulting from quarterly and from monthly data selection. Altogether the compared curves match well and thus indicate that the signal to noise level of the monthly mean stratospheric activities is still good enough to reflect real mean air mass mixing processes occurring on this timescale.

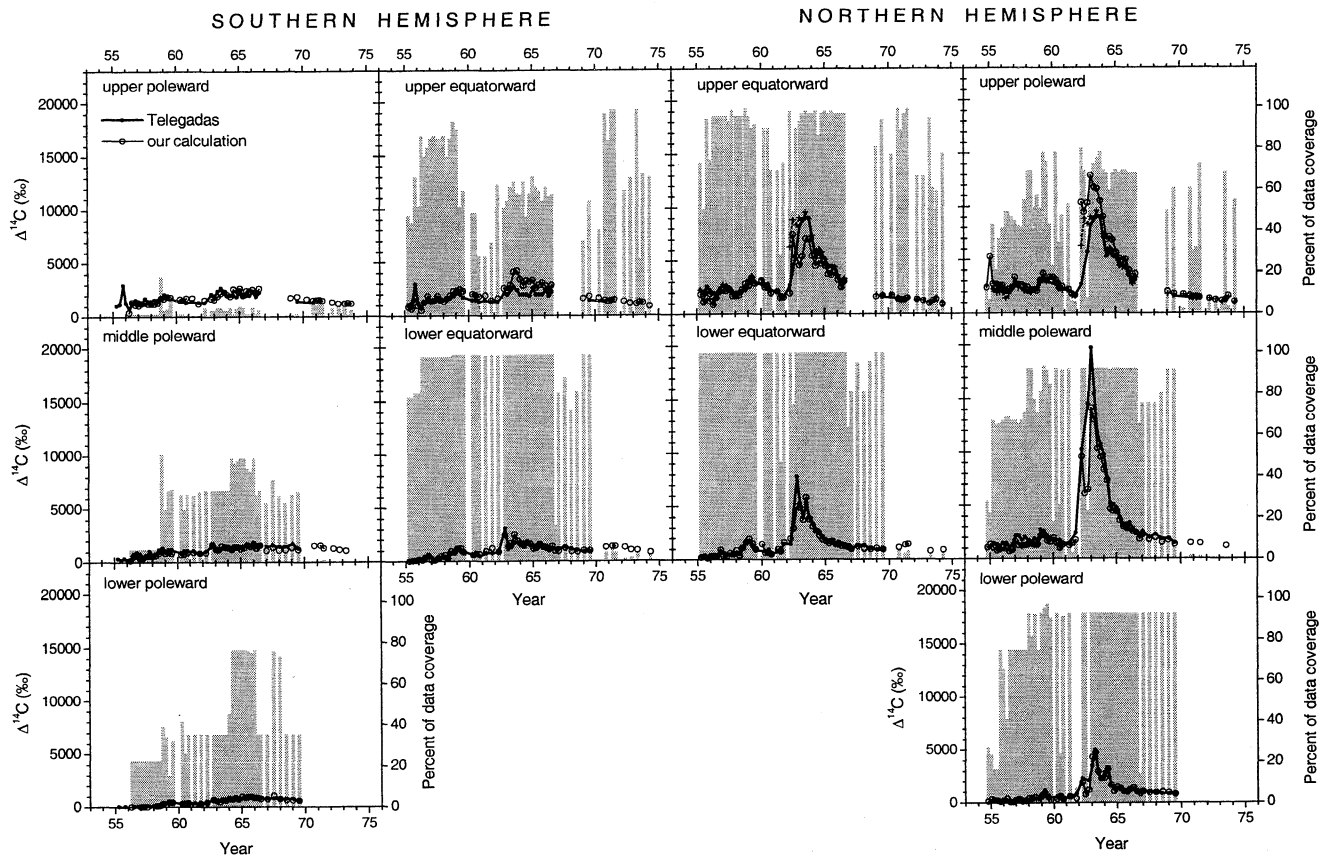

Figure 6. Comparison between our standard calculation of mean stratospheric $^{14}CO_2$ activities based on the HASL observations (thin lines with open circles) and the results published by *Telegadas* [1971] (thick lines with small solid circles). See Figure 4 for a description of the stratospheric subdivisions. The shaded bars represent estimates of the quarterly observational data coverage within each stratospheric subdivision (see section 3.1). Telegadas determined only the mean activity for the entire upper stratosphere of each hemisphere so that his results there have to be compared with the mean of our results for the upper poleward and the upper equatorward subdivisions in each hemisphere (dashed lines with crosses).

The expected smoothing down of predominant northern activity peaks reveals to be 20-30% in the lower stratosphere and only 10% in the middle poleward subdivision. In the upper northern stratosphere noise seems to prevail during 1962 and 1963, but this comes together with data coverage less than 50% (right axes in Figure 8) indicating that major parts of these subdivisions remained unobserved. Note the weak observational substantiation (less than 35% of monthly data coverage) of the highest monthly activity values in the northern upper equatorward subdivision toward mid-1962. This weak substantiation indicates that the peak in the corresponding quarterly mean which was already mentioned in section 3.1 may well be an artifact.

During the HASL survey latitudinal sampling in the Northern Hemisphere was concentrated near 10°N, 30°N, and 70°N apart from a period of intensive sampling between 1963 and 1967 (Figure 2b). To estimate the impact of latitudinal sampling density, we reject all observations located between 11°N and 29°N and between 35°N and 69°N from 1963 until 1967 and re-calculate mean stratospheric $^{14}CO_2$ activities. Figure 9 shows the results in the only three subdivisions where the rejection has some effect. A noticeable deviation is observed in the lower poleward subdivision and indicates that most of the information about the strong activity peak observed in 1964 was confined between 35°N and 70°N. Elsewhere the high-density latitudinal sampling adds remarkably little information with respect to mean $^{14}CO_2$ activities even during 1963 to 1964 when very high activity gradients passed through the stratosphere. This fact confirms the HASL observations as qualified to determine $^{14}CO_2$ inventories in the stratospheric subdivisions during periods of less intensive latitudinal sampling.

We also added Figure 10 to make clear that quarterly mean $^{14}CO_2$ activities determined for the high-altitude layer between 30 and 40 km are lower than mean activities found in the underlying upper stratospheric layers during a couple of years after the main bomb ^{14}C injections. This observational evidence contributes to refute the occasionally discussed hypothesis [*Johnston*, 1989; *Hesshaimer et al.*, 1994] that extremely high activities which correspond to major hot spots of bomb $^{14}CO_2$ residing in the very high stratosphere escaped the HASL network because it extended only up to 40 km.

Further sources of uncertainty in our $^{14}CO_2$ inventories may reside in a distinct sensitivity to isolated samples with particularly high or low ^{14}C activity. We test this impact by rejecting about 40% of the quarterly HASL observations before determining the $^{14}CO_2$ inventories with our standard procedure. The selection of the quarterly data in each subdivi-

Table 2. Results From Our Standard Calculation of Mean $^{14}CO_2$ Activities (See Figure 6) for the Stratospheric Subdivisions of Telegadas (See Figure 4).

Time,	Southern Hemisphere, dpm/g C							Northern Hemisphere, dpm/g C							
	Poleward				Equatorward			Equatorward			Poleward				
year	Lower	Middle	Upper	High	Lower	Upper	High	Lower	Upper	High	Lower	Middle	Upper	High	f
54.79	----	----	----	----	----	----	----	----	----	----	16.07	28.88	47.76	----	1.0015
55.04	----	----	----	----	----	----	----	----	----	----	18.83	33.04	88.52	----	1.0019
55.29	----	----	----	----	14.44	25.53	----	16.92	40.34	----	17.28	28.20	52.38	----	1.0024
55.54	----	----	----	----	14.98	23.21	----	18.25	30.18	----	16.55	25.12	52.25	----	1.0029
55.79	----	----	----	----	15.22	37.06	----	15.37	35.78	----	15.34	25.99	50.28	----	1.0033
56.04	----	----	----	----	16.49	27.74	----	18.33	31.60	----	16.67	28.33	50.36	----	1.0038
56.29	14.13	16.42	19.54	----	15.64	21.06	----	19.08	26.10	----	19.65	26.98	44.06	----	1.0043
56.54	13.87	21.46	32.86	----	19.20	31.95	----	18.44	35.56	----	15.05	23.53	45.17	----	1.0048
56.79	13.56	22.73	29.70	----	21.52	40.18	----	26.56	43.82	----	15.14	25.25	47.84	----	1.0052
57.04	14.04	18.73	28.91	----	15.65	33.63	----	19.11	45.45	----	17.45	36.38	60.81	----	1.0057
57.29	14.12	19.83	31.34	----	15.68	33.97	----	18.16	44.91	----	19.39	31.33	51.88	----	1.0062
57.54	14.07	22.01	32.74	----	18.03	40.14	----	22.31	46.45	----	16.08	30.59	51.30	----	1.0066
57.79	13.42	22.16	30.93	----	20.83	34.82	----	20.72	37.84	44.77	16.77	31.29	49.22	46.57	1.0071
58.04	13.42	21.79	31.18	----	22.39	33.06	----	25.60	37.64	----	20.19	32.79	48.18	----	1.0076
58.29	15.46	23.21	31.16	----	18.89	36.58	----	19.60	38.71	----	20.20	33.79	45.06	----	1.0080
58.54	15.84	25.90	32.45	----	27.28	40.74	----	29.18	46.10	----	21.18	32.08	44.75	----	1.0085
58.79	18.58	28.61	38.34	----	25.97	46.34	41.11	35.80	53.73	45.23	17.55	32.04	43.54	45.77	1.0091
59.04	17.63	25.61	37.82	----	30.36	46.87	----	40.50	50.81	----	22.70	43.85	57.41	----	1.0096
59.29	20.21	27.36	40.42	----	30.68	48.72	----	34.96	61.44	44.83	26.47	44.19	66.07	48.34	1.0101
59.54	20.16	25.57	39.71	----	25.93	46.69	----	27.54	54.39	46.89	21.71	37.03	57.45	50.19	1.0107
59.79	----	----	----	----	----	----	----	----	----	----	17.99	36.00	61.11	----	1.0114
60.04	----	----	----	----	----	----	----	34.42	58.43	----	----	41.23	61.01	----	1.0120
60.29	18.11	24.18	37.38	----	22.09	42.50	----	23.03	50.24	48.76	19.15	34.56	57.59	53.42	1.0127
60.54	18.31	24.84	35.47	----	23.74	41.09	----	23.32	48.75	49.94	22.57	27.84	47.11	52.60	1.0134
60.79	18.88	26.72	38.63	----	23.49	39.47	----	21.28	41.91	----	19.11	32.08	49.07	----	1.0141
61.04	----	----	----	----	----	----	----	----	----	----	----	----	----	----	1.0148
61.29	17.66	26.82	38.58	----	27.27	40.82	----	27.22	43.98	----	21.91	31.32	45.42	----	1.0154
61.54	----	----	----	----	----	----	----	25.03	35.80	----	----	34.23	39.73	----	1.0161
61.79	18.29	25.51	30.78	----	30.91	33.65	----	36.23	36.00	----	19.92	38.47	37.92	----	1.0167
62.04	----	----	----	----	----	----	----	----	----	----	----	----	----	----	1.0173
62.29	19.79	26.41	35.89	----	26.54	36.89	----	41.33	41.72	39.20	40.35	147.77	159.57	65.01	1.0178
62.54	----	----	----	----	----	----	----	54.97	118.64	57.35	24.88	100.21	147.28	61.37	1.0184
62.79	23.53	36.91	37.95	----	47.97	50.31	----	83.76	89.31	46.41	30.62	105.28	158.61	60.28	1.0189
63.04	21.65	31.25	36.51	----	33.55	48.40	----	82.53	77.97	41.77	74.59	212.35	194.92	66.33	1.0194
63.29	20.31	30.60	40.94	----	38.04	54.08	----	66.37	89.98	59.25	81.23	196.59	179.18	79.15	1.0199
63.54	23.00	35.10	44.69	----	49.24	71.48	----	96.01	112.84	82.53	56.31	158.71	177.15	75.96	1.0204
63.79	22.63	33.76	46.79	----	40.25	72.93	----	67.25	112.35	88.73	45.71	147.52	161.41	74.33	1.0209
64.04	24.65	33.37	43.40	----	36.84	61.66	----	57.97	90.82	73.57	46.78	130.72	140.57	87.22	1.0214
64.29	24.13	30.90	40.89	----	36.66	53.67	----	52.23	77.25	65.70	59.29	116.81	111.04	75.40	1.0219
64.54	25.63	33.87	50.51	----	38.22	60.31	----	45.30	83.40	75.67	37.48	79.01	114.10	75.67	1.0224
64.79	24.38	33.71	45.02	----	36.91	58.97	----	40.05	79.51	63.30	29.14	75.97	109.60	70.53	1.0229
65.04	27.60	31.95	51.37	----	30.53	60.68	----	38.18	77.23	65.15	34.80	75.77	93.60	70.76	1.0235
65.29	26.29	33.25	41.92	----	31.99	51.04	----	34.98	66.45	65.10	33.09	64.16	85.71	71.73	1.0240
65.54	26.91	36.15	48.30	----	36.20	54.13	----	37.91	64.98	69.64	28.81	56.29	83.68	74.25	1.0246
65.79	27.17	34.99	48.12	----	33.03	57.23	----	33.75	68.29	68.66	28.58	54.15	84.12	73.94	1.0252
66.04	26.24	35.50	49.66	----	31.84	53.34	----	33.58	59.11	64.91	31.52	53.72	70.31	67.88	1.0258
66.29	25.72	32.40	44.64	----	29.55	47.24	----	31.23	49.04	61.26	33.57	50.05	57.50	63.82	1.0264
66.54	24.87	35.92	50.65	----	33.14	54.08	----	31.81	57.41	61.54	28.48	48.16	65.55	63.60	1.0270
66.79	----	----	----	----	27.52	----	----	30.28	----	----	26.42	39.44	----	----	1.0277
67.04	24.54	29.09	----	----	27.14	----	----	27.75	----	----	29.07	45.31	----	----	1.0284
67.29	----	----	----	----	----	----	----	----	----	----	----	----	----	----	1.0291
67.54	28.54	33.24	----	----	31.01	----	----	31.00	----	----	27.33	38.78	----	----	1.0298
67.79	----	----	----	----	----	----	----	----	----	----	----	----	----	----	1.0306
68.04	24.33	29.72	----	----	27.00	----	----	27.74	----	----	27.28	41.51	----	----	1.0315
68.29	----	----	----	----	----	----	----	----	----	----	----	----	----	----	1.0323
68.54	23.12	29.89	----	----	26.71	----	----	27.39	----	----	27.96	34.85	----	----	1.0331
68.79	----	----	----	----	----	----	----	----	----	----	----	----	----	----	1.0342
69.04	22.70	32.97	38.51	----	28.35	36.90	----	28.49	36.70	----	27.12	37.85	42.69	----	1.0352
69.29	----	----	----	----	----	----	----	----	----	----	----	----	----	----	1.0363
69.54	22.41	30.48	40.37	----	27.94	39.68	----	27.01	38.30	40.05	24.90	32.65	39.71	40.04	1.0373
69.79	----	----	----	----	----	----	----	----	----	----	----	----	----	----	1.0383
70.04		----	----	----	----	----	----	----	----	----	----	----	----	----	1.0393
70.29	----	----	36.85	----	----	37.44	----	----	38.51	37.41	----	----	39.06	37.49	1.0404
70.54	----	----	----	----	----	----	----	----	----	----	----	----	----	----	1.0414
70.79	----	35.50	35.11	----	32.40	34.25	33.72	29.47	33.56	33.81	----	34.01	37.02	35.43	1.0423

Table 2. Continued

Time,	Southern Hemisphere, dpm/g C							Northern Hemisphere, dpm/g C							
	Poleward				Equatorward			Equatorward			Poleward				
year	Lower	Middle	Upper	High	Lower	Upper	High	Lower	Upper	High	Lower	Middle	Upper	High	f
71.04	----	----	35.30	----	----	33.28	34.09	----	32.30	33.60	----	----	35.26	----	1.0431
71.29	----	35.66	35.88	34.92	33.33	33.90	34.26	32.86	32.54	34.30	----	----	35.31	34.60	1.0440
71.54	----	32.39	35.00	34.09	33.25	34.93	33.64	33.68	34.89	33.44	----	33.90	34.91	34.80	1.0450
71.79	----	----	----	----	----	----	----	----	----	----	----	----	----	----	1.0461
72.04	----	----	----	----	----	----	----	----	----	----	----	----	----	----	1.0472
72.29	----	32.20	32.56	----	32.17	32.77	----	----	32.90	----	----	----	32.95	----	1.0483
72.54	----	----	----	----	----	----	----	----	----	----	----	----	----	----	1.0495
72.79	----	30.46	31.01	----	28.60	30.20	----	----	31.19	----	----	----	31.68	----	1.0507
73.04	----	----	----	----	----	----	----	----	----	----	----	----	----	----	1.0520
73.29	----	29.06	31.10	33.05	28.34	29.34	31.59	24.72	27.55	30.30	----	----	30.46	31.61	1.0532
73.54	----	----	31.65	----	----	31.53	----	----	31.29	----	----	30.47	31.32	32.91	1.0544
73.79	----	----	31.14	----	----	30.82	----	----	32.91	----	----	----	37.16	----	1.0552
74.04	----	----	----	----	----	----	----	----	----	----	----	----	----	----	1.0559
74.29	----	----	----	----	25.22	26.45	----	26.53	26.93	----	----	----	29.47	----	1.0566

The time value represents the middle of a quarterly subdivision as used by Telegadas (see introduction of section 3). The columns with header entitled "High" represent results for subdivisions between 30 and 40 km (see Figure 10) not considered by Telegadas. All ^{14}C activities are expressed in dpm/g C and can be converted to $\Delta^{14}C$ using equation (2). The parameter f in the rightmost column of the table is the ratio $C_{MLO}(t)/313$ where $C_{MLO}(t)$ expressed in ppm is the yearly mean CO_2 mixing ratio at Mauna Loa station [*Keeling and Whorf*, 1990] linearly interpolated for time (t) and 313 ppm is a constant CO_2 mixing ratio used in the HASL tables (see section 2.1). We used results from a carbon cycle model [*Hesshaimer*, 1997] matching the Mauna Loa curve and predicting $C_{MLO}(54.0) = 313$ ppm to determine the values of f before 1959. The parameter f combined with the standard factor of 5.64 (see section 2.1) and with the correction D of Table 1 allows to convert the mean activities of Table 2 from dpm/g C to 10^5 atoms/g air for each particular stratospheric subdivision. As an example, the mean $^{14}CO_2$ activity $A_{SLP}(t)$ in the southern lower poleward subdivision at time $t = 56.29$ is $A_{SLP}(56.29) = 14.13$ dpm/g C $= 14.13\times5.64\times(f(56.29)+D_{SLP}/313)\times10^5$ atoms/g air $= 79.6932\times(1.0043-0.2/313)\times10^5$ atoms/g air $= 79.985\times10^5$ atoms/g air.

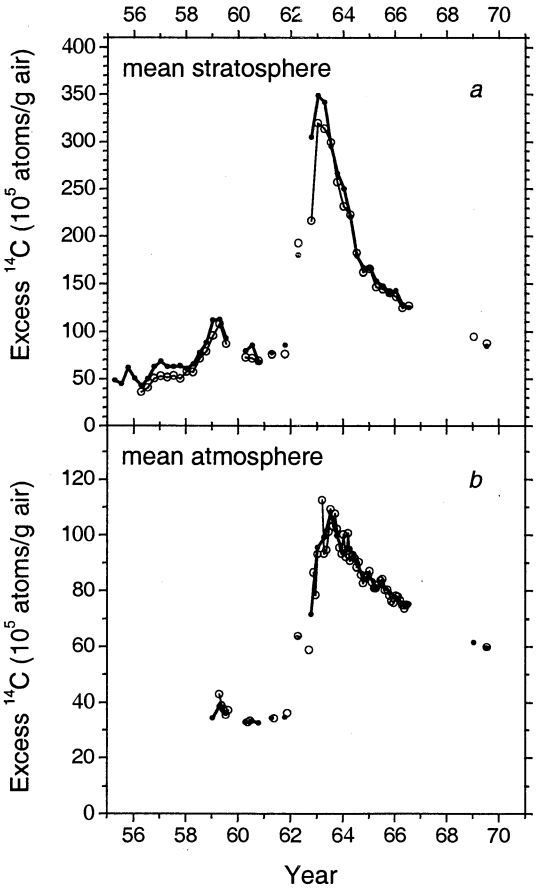

Figure 7. (a) Mean of the stratospheric $^{14}CO_2$ activities up to 30 km. The results of *Telegadas* [1971] (thick line with solid circles) are compared with the standard results of our new calculation (thin lines with open circles). The average difference μ between the results of Telegadas and our standard results is positive ($\mu = 7\times10^5$ atoms/g air) and the standard deviation of a single difference is $\sigma = 15\times10^5$ atoms/g air. (b) Mean of the atmospheric $^{14}CO_2$ activities up to 30 km. The quarterly mean results of our standard calculation (thick line with solid circles) are compared with the results (thin line with open circles) from our calculation with monthly resolution (see section 3.2.1). We used data from Wellington (41°S) [*Manning et al.*, 1990] in the Southern Hemisphere and data from Vermunt (47°N) [*Levin et al.*, 1985] in the Northern Hemisphere to determine the respective tropospheric ^{14}C inventories. The mean stratospheric activity values of Telegadas are obtained by division of his total stratospheric excess $^{14}CO_2$ inventories up to 30 km by the stratospheric air mass up to 30 km, which in his study is 1.02×10^{21}g. The mean stratospheric (resp. atmospheric) activity values from our standard and monthly calculations were obtained by division of our total stratospheric (atmospheric) excess inventories up to 30 km by the stratospheric (atmospheric) air mass up to 30 km in our study which is 1.06×10^{21}g (5.1×10^{21}g). Note that our standard and monthly activities in this figure also account for increasing CO_2 mixing ratios (see caption of Table 2), whereas the activities of Telegadas assume a constant CO_2 mixing ratio of 313 ppm.

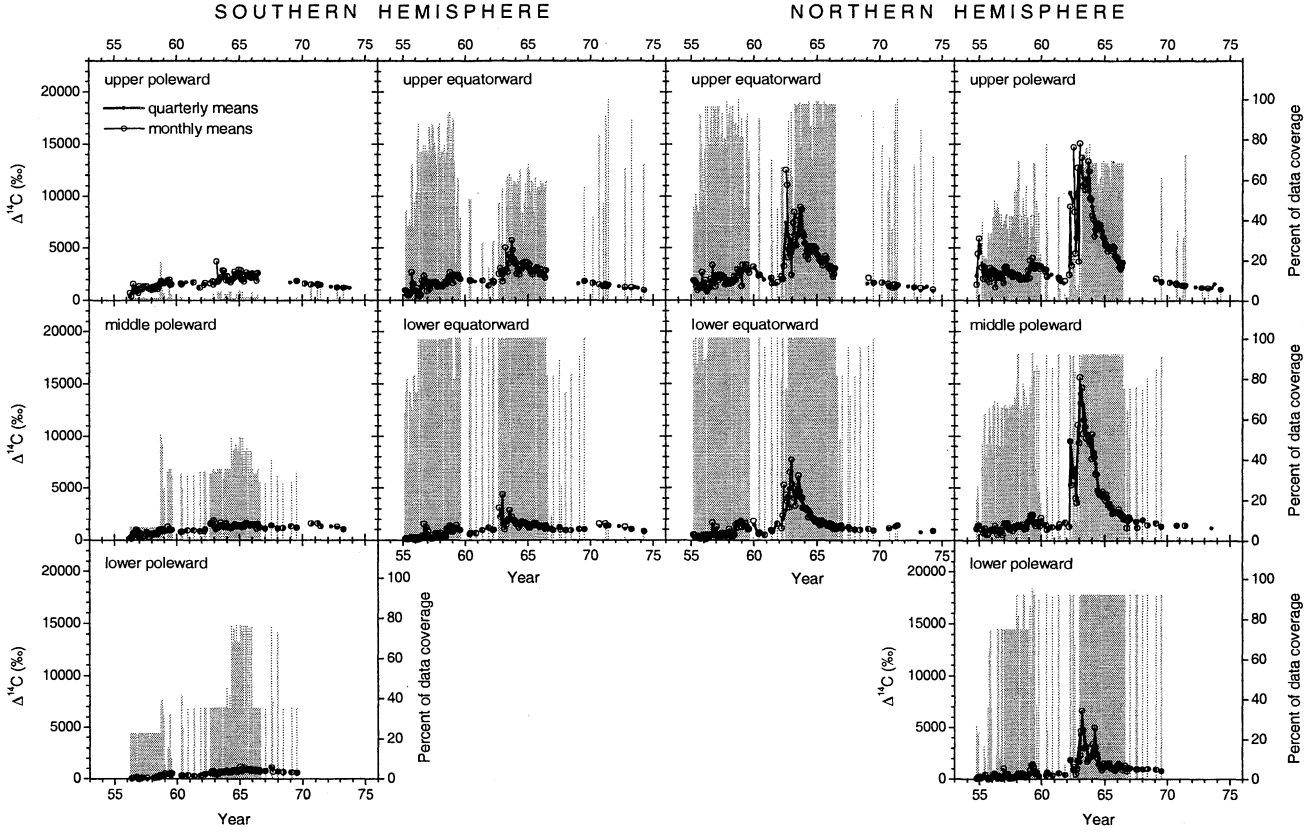

Figure 8. Comparison between our standard calculation of mean stratospheric $^{14}CO_2$ activities using quarterly means of the HASL observations (thick lines with small solid circles) and a calculation with higher, monthly mean time resolution (thin lines with open circles). The shaded bars represent estimates of the monthly observational data coverage within each stratospheric subdivision (see section 3.1).

sion consists in successively rejecting the two data points with the highest and the lowest ^{14}C activity up to a rejection of 40% of the quarterly subdivision data. The results reported in Figure 11 demonstrate the impressive robustness of the HASL data. Apart from missing peak activities during 1962 in the northern middle poleward and upper subdivisions, no significant deviation from $^{14}CO_2$ inventories based on the entire HASL observation set is found.

In our standard calculation we use all data from the HASL reports except number 1216 [*Hagemann et al.*, 1965] for which the latitude is missing and number 3383 [*Hagemann et al.*, 1966] sampled during November 1962 at 8°N and 18 km height which has a corrected specific activity of 748.5 dpm/g C ($\Delta^{14}C$ = 52223‰). This activity is the highest of the HASL reports and lies 5 to 10 times higher than in other samples collected at that location and time. We decided to use all other HASL data, although some 450 activity values tabled in reports 159, 166, 174, 214, and 242 are marked as "less reliable." This mark is due (1) to the absence of a $\delta^{13}C$ value and to a CO_2 mixing ratio greater than 389 ppm, (2) to the absence of corrections by either the CO_2 mixing ratio or $\delta^{13}C$ methods, (3) to positive $\delta^{13}C$ values, or (4) to the absence of CaO purification during sample preparation. We find no noticeable impact of these samples when calculating the mean stratospheric $^{14}CO_2$ activities obtained after rejection of the less reliable data and comparing these activities with results obtained in our standard calculation. The resulting differences between the curves are so small that we refrain from showing them in a figure.

3.2.2. Errors due to interpolation. We base our interpolation procedure on Delaunay triangulation which has a well-developed theory [*O'Rourke*, 1994] and allows linear interpolation based on only one a priori parameter. Our Delaunay triangle mesh structure is set up in the two-dimensional height versus latitude diagram and depends on the a priori choice of coordinate system units. In the particular geometry of our study dealing with air mass exchange, the "distance" between points would be ideally expressed as the mean time needed for a concentration pulse to propagate from one point to the other. We take this into consideration when determining the triangulation mesh by re-scaling linearly the height between 0 and 40 km to the interval $Y \in [0,2]$ which has a length of 2 and the latitude between 90°S and 90°N to the interval $X \in [-0.5,0.5]$ which has a length of 1. This y/x scale ratio of 2/1 reflects very roughly the fact that meridional air mass exchange in the stratosphere takes about 1 to 2 years, whereas vertical air mass exchange takes about twice as long. We estimate the impact of different choices of y/x by comparing the standard results obtained using a ratio of 2/1 with the results obtained using ratios of 8/1 or 1/2. The resulting curves show only minor differences between the different curves, and we do not show them in a figure. These changes in technique produce an average difference μ between the results obtained using a ratio of 8/1 (respectively, 1/2) and our standard result which is positive ($\mu = 2\times10^5$ atoms/g air) (respectively, negative ($\mu = -0.3\times10^5$ atoms/g air)). The standard deviation of a single difference is $\sigma = 4\times10^5$ atoms/g air (respectively, $\sigma = 6.1\times10^5$ atoms/g air) (μ and σ were

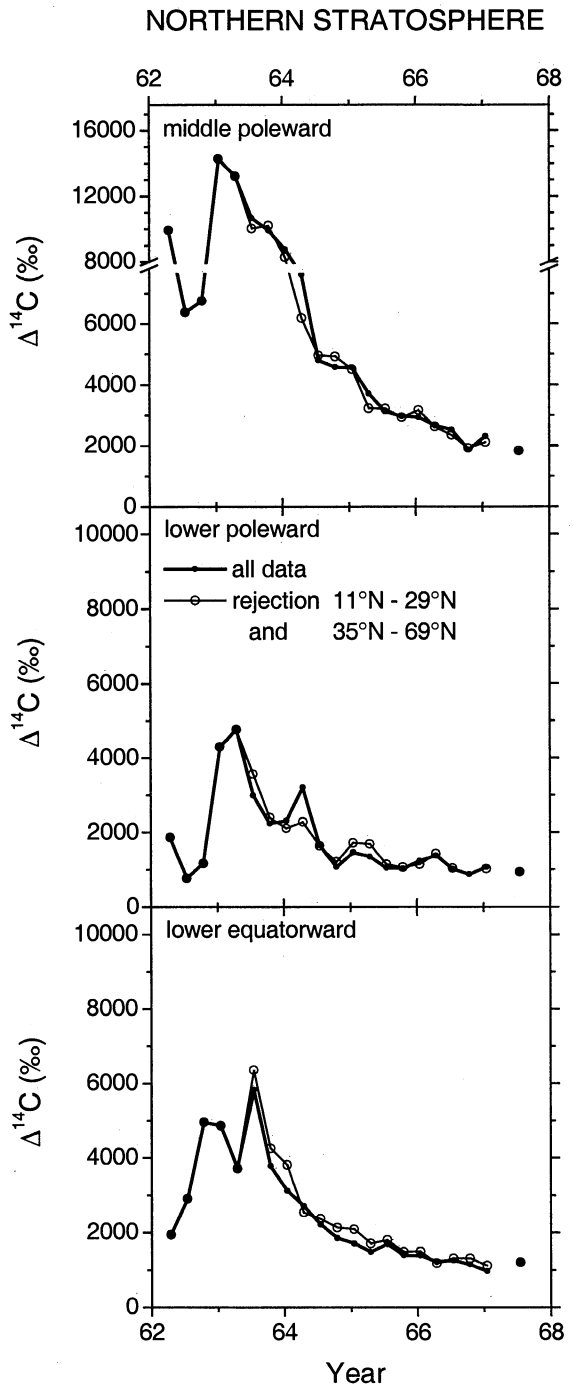

Figure 9. Comparison between our standard calculation of mean $^{14}CO_2$ activities in stratospheric subdivisions of the Northern Hemisphere using all HASL observations (thick lines with small solid circles) and the results obtained when rejecting the HASL observations sampled between 11°N and 29°N and between 35°N and 69°N from January 1963 to January 1967 (thin lines with open circles).

determined in a similar way as described in the caption of Figure 7).

In our standard calculation the activity inside a given Delaunay triangle is a linear function of latitude and height chosen to fit the activity values at the three coordinates generating the Delaunay triangle. The choice of a low-order linear interpolation method may be a concern about data including sharp peaks. We estimate the uncertainty attributable to this impact by using a Delaunay triangle based cubic method [*Yang*, 1986; *Watson*, 1994] to determine the mean $^{14}CO_2$ activities in all stratospheric subdivisions. The resulting curves match the standard results without noticeable deviation, and we refrain from showing them in a figure. This change in technique produces an average difference μ between the results obtained using a cubic method and our standard results which is negative (μ = -2.3×10^5 atoms/g air). The standard deviation of a single difference is σ = 4.7×10^5 atoms/g air (μ and σ were determined in a similar way as described in the caption of Figure 7).

Actually, a Delaunay mesh is only one among a multitude of possible triangulations for a given set of points. We showed before that differences in the Delaunay mesh due to variations of the *y*/*x* scale ratio within a physically reasonable range produce only negligible deviations between the resulting mean $^{14}CO_2$ activities. We further test the impact of a different although still reasonable triangulation on the obtained mean $^{14}CO_2$ activities by defining new sets of quarterly points basing on the first standard Delaunay triangulation (see Figure 5b). The new points are located in the middle of each segment belonging to the standard triangulation. The activity of each new point is simply the mean activity of its segment extremities. This generates a new, about 2 to 3 times as numerous set of quarterly activity points on which we apply the standard triangulation and integration procedures to determine mean $^{14}CO_2$ activities. The results reported in Figure 12 agree well with the curves from our standard calculation. The strongest differences are found in the northern stratosphere during 1962 and 1963 when activity passes only through one predominant peak in the lower equatorward subdivision and shows a more pronounced indentation in the upper poleward subdivision. A further difference is found in the northern upper equatorward subdivision where activities between mid-1963 and mid-1966 remain about 10% below the standard calculation.

4. Comparison Between the HASL Data and Observations From Other Authors

Sampling locations from other sources than the HASL reports are also shown in Figure 2. These independent data sets allow to check how far their $^{14}CO_2$ activities agree with the HASL observations. We subdivide our investigation into three parts and start with a section summarizing activity measurement errors in the HASL data. The second and third sections are devoted to activity comparisons in the troposphere and in the stratosphere.

4.1. Activity Measurement Errors

CO_2 contamination effects are minimized in the HASL activities by applying either a ^{13}C-based correction when $\delta^{13}C$ measurement exists or a crude CO_2 concentration-based correction when only that concentration measurement is available [*Hagemann et al.*, 1965]. Figure 13 shows that about 40% of the uncorrected activities lie within 1% of the corrected activity values and that about 85% of the uncorrected activities lie within 10% of the corrected activity values. Note in Figure 13c that the corrections applied to high activities tend to be smaller than those applied to low activities.

The value of activity counting errors given in the HASL reports 159, 166, 174, 214, and 242 is represented statistically

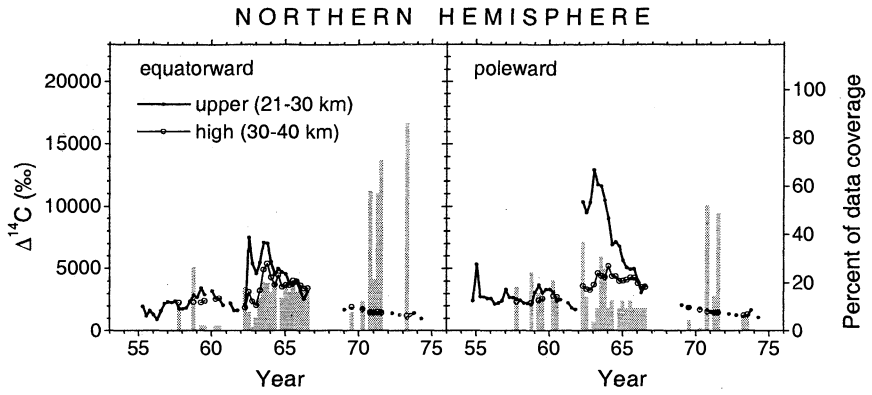

Figure 10. Comparison between quarterly mean $^{14}CO_2$ activities determined for the upper (thick lines with solid circles) and for the high (thin lines with open circles) stratospheric subdivisions of the Northern Hemisphere using our standard calculation based on HASL data. The shaded bars represent estimates of the quarterly observational data coverage (see section 3.1) within the high stratospheric subdivision. See Figure 4 for a description of the stratospheric subdivisions.

in Figure 14. The relative activity errors lie most frequently between 1% and 2%. Only 1/20 of the relative errors are larger than 5% and about 1/5 of the errors are larger than 3%. In HASL reports 246, 284, and 294 [*Telegadas et al.*, 1972; *Sowl et al.*, 1974, 1975], counting errors of the observed activities at the 95% confidence level are declared smaller than 5% in all samples and smaller than 3% in 90% of the samples. Figure 14c also shows that for activities with $\Delta^{14}C$ higher than 1000‰ which essentially contribute to the high bomb $^{14}CO_2$ inventories in the northern hemispheric strato-

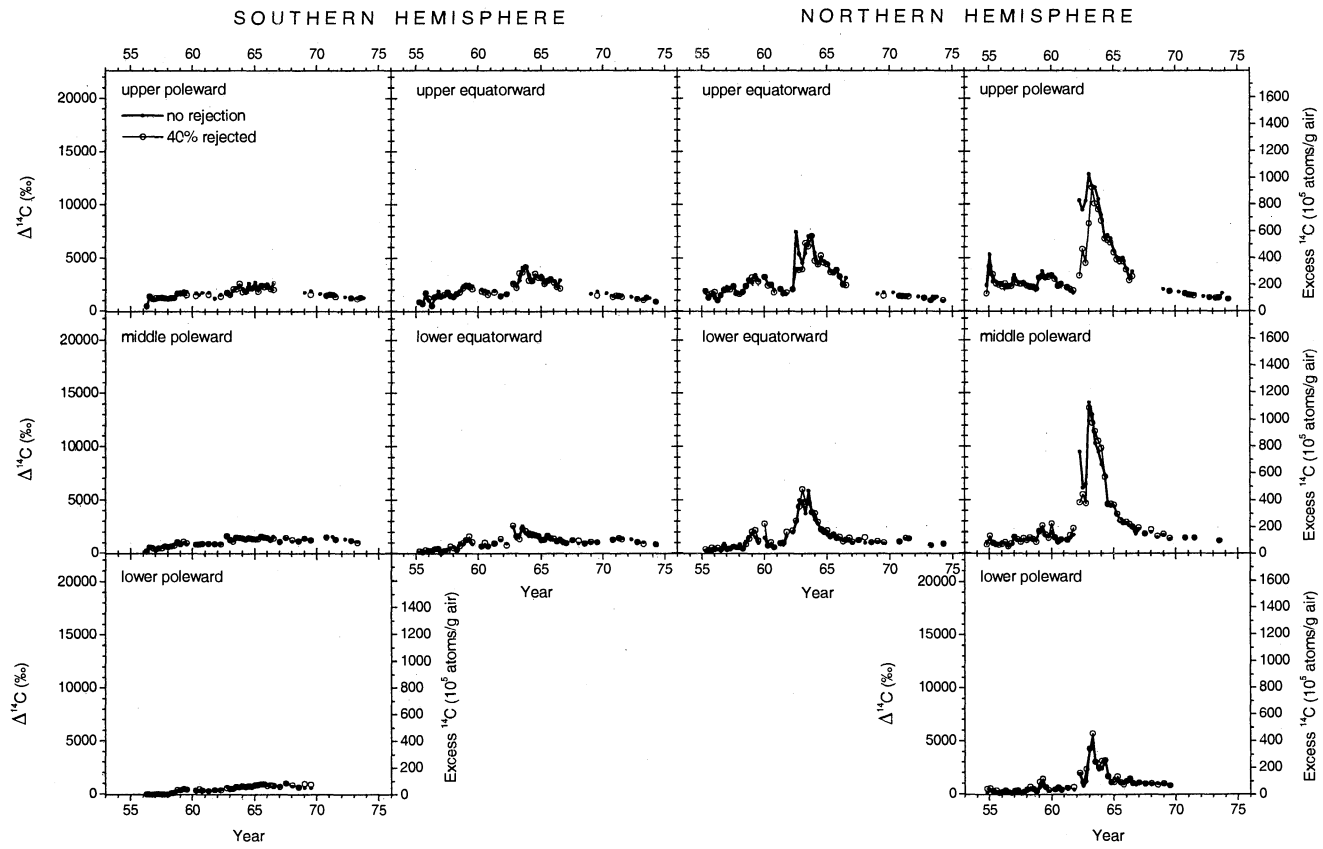

Figure 11. Comparison between our standard calculation of stratospheric bomb $^{14}CO_2$ activities based on all HASL observations (thick lines and small solid circles) and the results obtained after rejection of 40% of the observations (thin lines with open circles). The mean activity in the stratospheric subdivisions is expressed in the Δ scale on the left-hand sides of the figure and in units of 10^5 excess ^{14}C atoms per gram of air on the right-hand sides. The activity scale conversion and the rejection procedure are explained in sections 2.1. and 3.2.1.

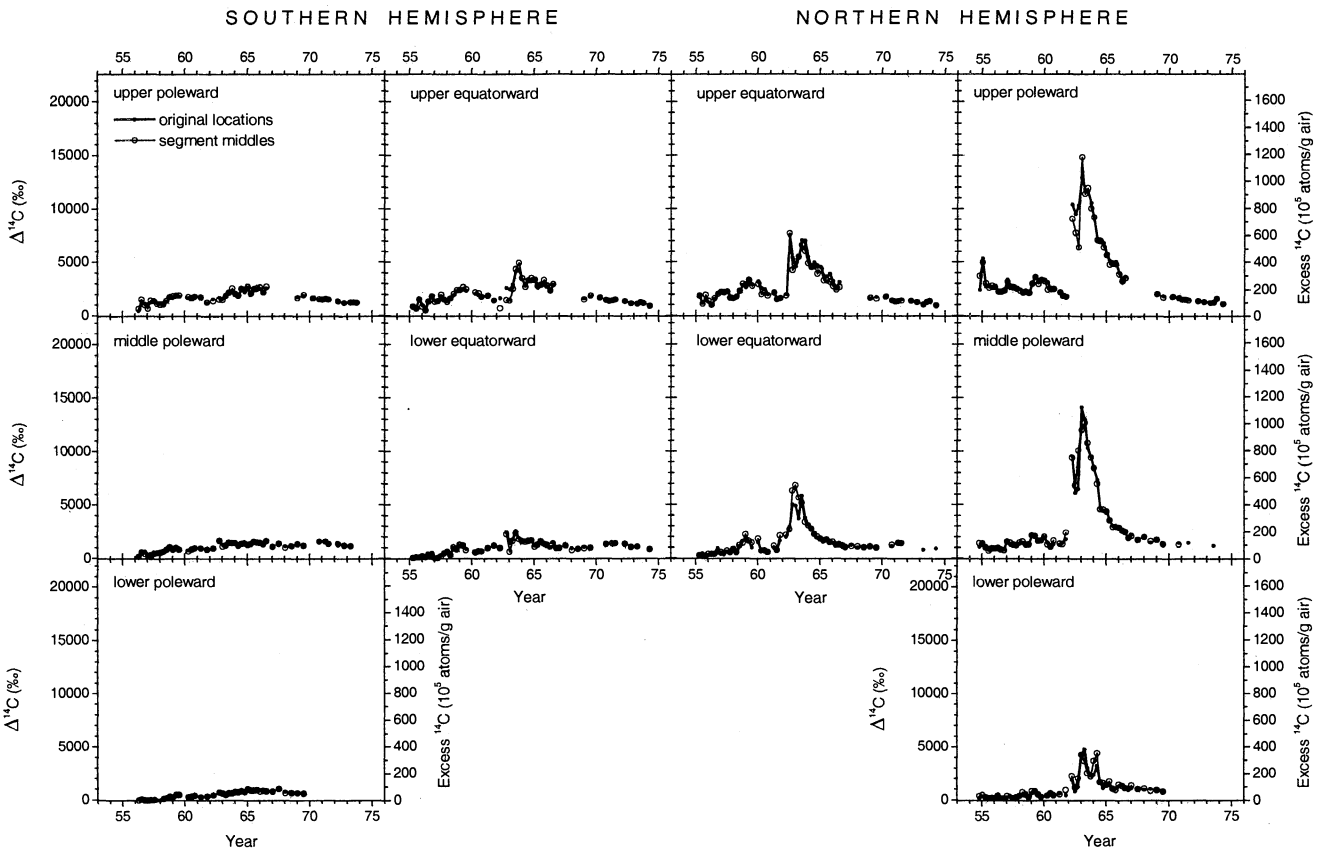

Figure 12. Comparison between mean $^{14}CO_2$ activities from our standard calculation based on Delaunay triangulation of the original quarterly collected HASL observations (thick lines with solid circles) and the results obtained when constructing the triangulation on the middles of the standard Delaunay triangle segments. The mean activity in the stratospheric subdivisions is expressed in the Δ scale on the left-hand sides of the figure and in units of 10^5 excess ^{14}C atoms per gram of air on the right-hand sides. See section 3.2.2 for a description of the triangulation based on segment middles and Figure 5b for an example of this triangulation.

sphere (see, e.g., Figure 6), the relative errors are most frequently much smaller than the upper limits mentioned above. As the quarterly mean $^{14}CO_2$ activity of each stratospheric subdivision is usually based on at least 4 and up to 100 or more observational points, the relative uncertainty on bomb $^{14}CO_2$ inventories due to counting errors is expected to be less than 1%.

Concerning our mean $^{14}CO_2$ activities in stratospheric subdivisions, we deduce from the preceding discussion that the relative uncertainties originating from both contamination and counting errors are less than a couple of percents. One could expect from corrections and errors drawn in Figures 13c and 14c that these uncertainties may sensibly increase after 1966 when corrections and counting errors could rise due to decreasing $^{14}CO_2$ activities. We therefore included separate statistics for the stratospheric HASL data after 1966 in Figures 13 and 14 (shaded, still from reports 159, 166, 174, 214, and 242 only) to demonstrate that this assumption is erroneous.

4.2. Comparison Between HASL and Other Observations in the Troposphere

In his paper devoted to stratospheric bomb $^{14}CO_2$ inventories, *Telegadas* [1971] called the quality of HASL activities into question when comparing surface station excess $^{14}CO_2$ activities from other sources than HASL reports with the excess activities from HASL samples collected near ground level (<5 km) aboard aircraft which he found to be mostly higher by 5-20%. Telegadas suggested from this apparent discrepancy that, for unknown reasons, the calibration of low-altitude excess $^{14}CO_2$ activities from HASL reports may be too high by up to 20%. From this conclusion and comparison with high-altitude measurements from *Ergin et al.* [1970], *Tans* [1981] inferred that possibly all HASL excess activities are 20% too high. We, however, do not actually understand these conclusions which generally devaluate the unique HASL database. Neither the activity corrections reducing contamination effects nor the activity counting errors allow such a large systematical bias. Furthermore, the aircraft samplings took place very likely in daylight when vertical convection is much stronger than at night. Hence during a period of strong stratospheric bomb $^{14}CO_2$ sources, we expect that the lower hull of low-altitude activities from spot samples collected aboard aircraft during 1-2 hours matches activities from samples integrated at ground level stations during several days and we argue that precisely this behavior is reflected in Figure 15.

4.3. Comparison Between HASL and Other Observations in the Stratosphere

Figure 15 also shows how far the variability of $^{14}CO_2$ activity in tropospheric aircraft samples reflects the high

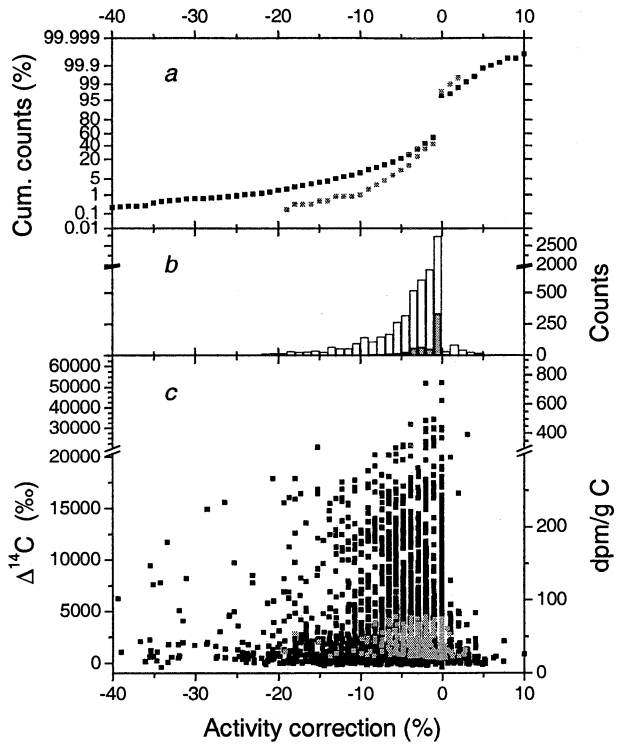

Figure 13. Statistical representation of $^{14}CO_2$ activity corrections performed in the HASL reports 159, 166, 174, 214, and 242 on uncorrected activities A_{uncorr} (dpm/g C) to obtain corrected activities A_{corr} (dpm/g C) accounting for contamination effects. In Figure 13c the corrected activity A_{corr} is reported versus the relative activity correction $(A_{uncorr}-A_{corr})/A_{corr}$ expressed in percent. In the last formula the activity correction is expressed relatively to the corrected activity to simplify the discussion on uncertainties of the corrected activities. Note that the vertical patterns only reflect the numerical rounding used in the HASL tables. Bars in Figure 13b represent the number of data points which relative activity correction lie within a given interval of 1%. The cumulative number of data points with a relative activity correction smaller than the abscissa value is reported in Figure 13a. Solid squares, and open bars represent the entire data set, whereas shaded squares and shaded bars refer to the part of the observations sampled in the stratosphere after January 1966. The activity is expressed in the Δ scale on the left-hand side of Figure 13c and in dpm/g C on the right-hand side.

activity in the overlying stratospheric layers. The figure incidentally makes clear how difficult it is to compare few spot samples during periods of high activity gradients. This remains true for the stratospheric observations of *Ergin et al.* [1970] cited by *Tans* [1981] which are essentially the same as those presented by *Walton et al.* [1970] and shown in Figure 2 except that the latter publication reveals individual latitudes for each sampling location. They were sampled during 1967 and 1968 between 50°N and 60°N where no HASL observations were available at that time of low latitudinal sampling density (see Figure 2b). Hence a quantitative comparison between the observations from Ergin et al. and HASL data remains questionable because it depends substantially on interpolation assumptions at a location with pronounced activity gradients. We illustrate our reasonable doubt in Figure 16 comparing the data from *Walton et al.* [1970] and from *Nydal and Lövseth* [1983] sampled between 11 and 13 km height with HASL observations collected aboard aircraft during the same periods (see Figure 2). Comparable HASL data at the time of the Walton et al. sampling are concentrated only in two narrow intervals ranging from 30°N to 40°N and from 70°N to 80°N. Apparently, a relative increase of excess activities from Walton et al. by about 20% would better fit in Figure 16 between the lower activities at 30°-40°N and the higher activities at 70°-80°N. One could argue that the same is true for excess activities from Nydal and Lövseth as well as for the activity values marked with pluses in Figure 16 and conclude that all excess activities of the HASL reports are about 20% too high. The fact that the activity values marked with pluses are themselves HASL report data demonstrates the weakness of this kind of argumentation.

Unfortunately, the sampling locations found in the HASL reports differ too much from those in the other available sources cited in the present paper to allow direct comparison of the respective $^{14}CO_2$ activities. However, the positive about

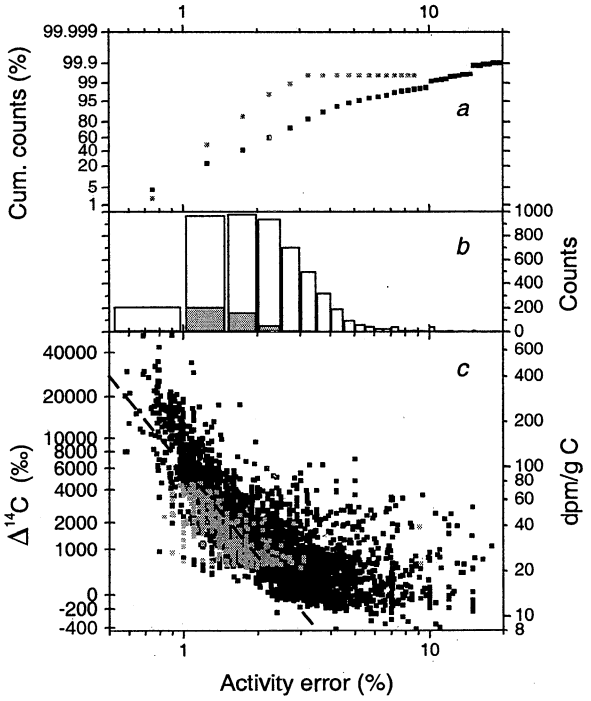

Figure 14. Statistical representation of counting errors listed for $^{14}CO_2$ activities in the HASL reports 159, 166, 174, 214, and 242. An activity error of $\varepsilon = 1\%$ for an activity A means that the real activity lies at the 95% confidence level in the inverval $[(1-\varepsilon)\ A\ ,\ (1+\varepsilon)\ A]$. In Figure 14c the corrected activity (see Figure 13) is reported versus the activity counting error expressed in percent of the corrected activity. Discernible vertical patterns only reflect the numerical rounding used in the HASL tables. A dashed line is added to show the slope of a fictive error function increasing with the square root of the activity. Bars in Figure 14b represent the number of data points which activity error lie within a given interval of 0.5%. The cumulative number of data points with an activity error smaller than the abscissa value is reported in Figure 14a. Solid squares and open bars represent the entire data set, whereas shaded squares and shaded bars refer to the part of the observations sampled in the stratosphere after January 1966. The activity is expressed logarithmically in dpm/g C on the right-hand side of Figure 14c and in the corresponding Δ scale on the left-hand side.

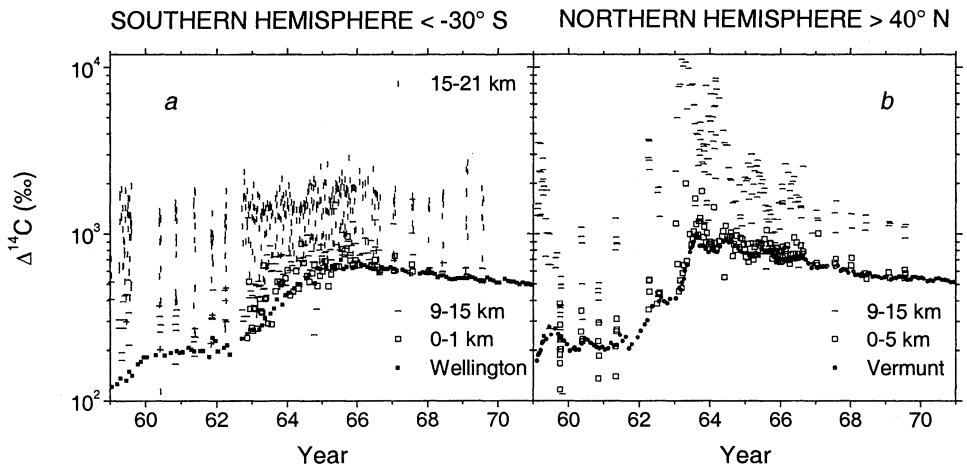

Figure 15. Comparison between $^{14}CO_2$ activities from aircraft spot samples collected during 1-2 hours as published in the HASL reports and observations from basic solution samples integrated over several days at the ground level stations Wellington (41°S) [*Manning et al.*, 1990] and Vermunt (47°N) [*Levin et al.*, 1985]. (a) Wellington station data (solid squares) are compared with the aircraft observations sampled south of 30°S successively at altitudes lower than 1 km (open squares), between 9 and 15 km (horizontal bars) and between 15 and 21 km (vertical bars). (b) Vermunt station data (solid circles) are compared with aircraft data sampled north of 40°N, mostly between 70°N and 80°N successively at altitudes lower than 5 km most frequently located between 4 and 5 km (open squares) and at altitudes between 9 and 15 km (horizontal bars).

it is that the mentioned observations from other sources fill optimally some lacunas of the HASL survey. Hence embedding these other observations in the HASL data constitutes a further test of robustness for the calculated mean $^{14}CO_2$ activities. Due to the particular location of these supplementary data the most significant impacts are expected in the northern hemispheric stratosphere. Figure 17 illustrates this fact and shows that the only differences of interest are found

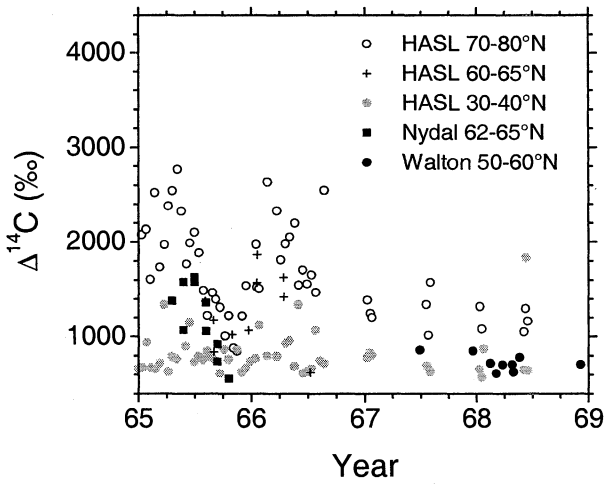

Figure 16. Subset of $^{14}CO_2$ activities sampled at altitudes between 11 and 13 km using aircraft. The data from *Walton et al.* [1970] (solid circles) sampled between 50°N and 60°N and the data from *Nydal and Lövseth* [1983] (solid squares) sampled between 62°N and 65°N are compared with HASL observations sampled between 30°N and 40°N (shaded circles) and between 70°N and 80°N (open circles). The data from Nydal and Lövseth were mostly sampled at 12 km height and are also compared with a few HASL samples (pluses) collected from mid-1965 to mid-1966 between 60°N and 65°N at comparable altitudes (13 km).

in the lower poleward subdivision where systematical deviations are only found after early 1962. About 5-10% lower values than the standard activity are found between late 1962 and late 1963 as well as between mid-1967 and early 1969, respectively, when the samplings from *Godwin and Willis* [1964] and from *Walton et al.* [1970] took place between 50°N and 60°N in the vicinity of the British Isles (see Figure 2b). We emphasize that these lower values are not a compelling proof for inaccuracies in the HASL activity measurements but can be reasonably interpreted as a consequence of the $^{14}CO_2$ activity being a nonlinear function of location. A further interesting feature of the enlarged data set is the completion of an activity peak in the northern lower poleward stratosphere during early 1965 when the sampling from *Berger et al.* [1965] took place over the continental United States and the Caribbean. The stronger peak seems to fit much better than the standard calculation into a decreasing sequence of seasonal $^{14}CO_2$ activity peaks observed after 1963 which result from the seasonally variable cross-tropopause air mass exchange. Although weakly substantiated by only two observational data, this peak completion confirms the fact already noticed in 3.2.1 that ^{14}C evidence for the seasonal variation of cross-tropopause air mass exchange is mainly confined between 30°N and 70°N.

5. Conclusions

The $^{14}CO_2$ activities published in the HASL reports turn out to be an uncut diamond among modern geophysical observations. We have shown that the interpretation of these data compiled to produce mean stratospheric $^{14}CO_2$ activities is robust and stands not only the test of various numerical integration assumptions but also brute force attacks like rejecting 40% of the data. Therefore both the distinct behavior of the predominant activity excursions in the different stratospheric subdivisions as well as more subtle seasonal patterns detectable in the northern stratosphere after 1963 cry out for

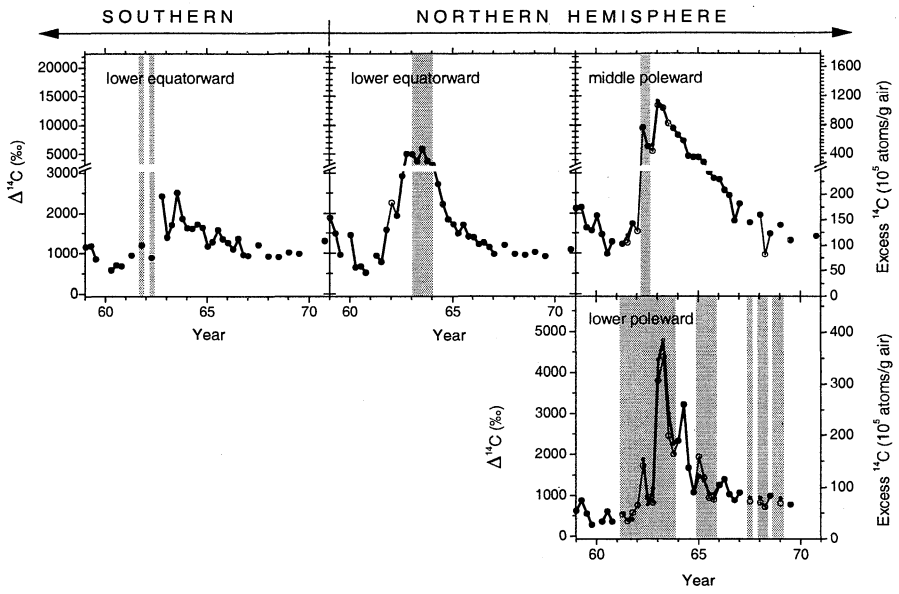

Figure 17. Mean $^{14}CO_2$ activity (open circles and thin lines) calculated for our stratospheric subdivisions when using HASL data together with observations from *Fergusson* [1963], from *Godwin and Willis* [1964], from *Berger et al.* [1965], from *Walton et al.* [1970], and from *Nydal and Lövseth* [1983] (see Figure 2). The figure shows the deviation from results of our standard calculation using only HASL data (thick lines and solid circles). Shaded areas indicate periods when non-HASL data were collected within a stratospheric subdivision. The activity is expressed in the Δ scale on the left-hand sides of the figure and in units of 10^5 excess ^{14}C atoms per gram of air on the right-hand sides.

interpretation in terms of inner stratospheric and cross-tropopause air mass transport. We will present (V. Hesshaimer and I. Levin, manuscript to be submitted to Journal of Geophysical Research, 2000) corresponding first-order results coming out of a carbon cycle simulation including a simple atmospheric compartment model in which the air mass transport parameters are adjusted to optimally match the mean stratospheric $^{14}CO_2$ activities of the present study. We have also shown that the signal to noise ratio in the HASL activities is good enough, not only on the quarterly but also on the monthly timescale. This indicates that many valuable details (see, e.g., the relaxation time of about 1 month from peak activities to stratospheric background repeatedly shown in Figure 1) are buried in these data which will allow to sound out the reality of global scale air mass transport in atmospheric three-dimensional models.

We reasonably dissipated several doubts regarding lacunas of the HASL survey and pretended inadequacies of the corresponding activity measurement. Hence only two main points of objections remain concerning the validity of stratospheric bomb $^{14}CO_2$ inventories based on this survey. The first point emphasizes the fact that some hot spots of bomb $^{14}CO_2$ may have been missed because of the limited observational network. *Telegadas* [1971] used this argument to explain why his $^{14}CO_2$ inventories do not reflect some Chinese nuclear tests, but we analyzed an example at the end of section 3.1 where this criticism turned out to be inappropriate. Also *Tans* [1981, Figure 3] used that argument to explain why his quarterly mean atmospheric inventory of bomb $^{14}CO_2$ up to 30 km increased until mid-1963 although the last major nuclear tests and the corresponding maximal activities in the stratosphere (Figure 7a) took place around Christmas 1962 before the Test Ban Treaty became effective. The problem is confirmed by the quarterly mean atmospheric $^{14}CO_2$ activities determined from our standard calculation (Figure 7b). Note that the monthly mean atmospheric activities in Figure 7b show their highest value already in March 1963, but activities in April and in May are inconsistently lower so that a more refined analysis would be needed to determine whether the higher or the lower monthly mean activity levels are better substantiated by the observations. Hence the present state of our revision confirms *Tans* [1981] arguing that some bomb ^{14}C was missed during a couple of months after the cessation of nuclear testing. The argument appears to be quite reasonable because corresponding nuclear detonations took place at 75°N over the former Soviet Union, whereas the HASL network extended only up to 73°N. The missed ^{14}C has most probably resided within a narrow polar stratospheric cap because we already refuted in section 3.2.1 that major bomb $^{14}CO_2$ hot spots located above 40 km escaped the HASL network. Except for this weakness, our mean $^{14}CO_2$ activities calculated using interpolation only inside the convex hull of sampling locations are confirmed to be good estimates of mean $^{14}CO_2$ activities for the entire stratospheric subdivisions.

The second point of objection queries the fundamental working hypothesis which considers that the HASL observations represent valid longitudinal means of the $^{14}CO_2$ activity. We already presented evidence in favor of our working hypothesis in section 2.2 in a comparison between HASL observations sampled over the British Isles and HASL observations sampled over the United States. In addition, we have shown results of our calculation obtained after embedding observations from *Godwin and Willis* [1964] and from *Walton et al.* [1970] into the HASL observations to compute mean stratospheric $^{14}CO_2$ activities (see section 4.3). Also these results do not reveal important longitudinal effects coming from the fact that the former observations were sampled over the British Isles, whereas the corresponding HASL sampling

took place over the United States and the Pacific Ocean. In summary, it may be said that despite our attempts we found no serious reason to call our fundamental working hypothesis into question.

The uncertainty attributable to our quarterly mean stratospheric $^{14}CO_2$ activities was found to be usually less than ±5% exception made of isolated sequences mentioned in the text where it can amount to 10% or exceptionally to 20% or more in particular activity peaks or indentations. Some of these uncertainties can be further reduced by ensuring consistent conservation of the number of ^{14}C atoms during the interplay of $^{14}CO_2$ exchange within the stratosphere and across the tropopause. Doing this requires realistic simulation of both the bomb ^{14}C input and of ^{14}C following the paths of the global carbon cycle of which, as counterpart, our understanding will be seriously challenged by the present rehabilitation of stratospheric bomb $^{14}CO_2$ observations.

Acknowledgments. We owe much to the scientists who understood the importance of making careful global-scale atmospheric measurements over long time spans and who carried out the measurements published in the HASL reports. This work was supported through grants from the European Commission (contracts EV5V-CT92-0120 and ENV4-CT95-0116).

References

Ashenfelter, T.E., J. Gray Jr., R.E. Sowl, M. Svendsen, and K. Telegadas, A lightweight molecular sieve sampler for measuring stratospheric carbon-14, *J. Geophys. Res., 77*(3), 412-419, 1972.

Berger, R., G.J. Fergusson, and W.F. Libby, UCLA radiocarbon dates IV, *Radiocarbon, 7*, 336-371, 1965.

Broecker, W.S., and T.-H. Peng, Stratospheric contribution to the global bomb radiocarbon inventory: Model versus observation, *Global Biogeochem. Cycles, 8*(3), 377-384, 1994.

Broecker, W.S., S. Sutherland, W. Smethie, T.-H. Peng, and G. Östlund, Oceanic radiocarbon: Separation of the natural and bomb components, *Global Biogeochem. Cycles, 9*(2), 263-288, 1995.

Enting, I.G., K.R. Lassey, and R.A. Houghton, Projections of future CO_2, *CSIRO DAR Tech. Pap. No. 27*, Div. of Atmos. Res., Commonw. Sci. and Ind. Res. Org., Mordialloc, Australia, 1993.

Ergin, M., D.D. Harkness, and A. Walton, Glasgow University radiocarbon measurements II, *Radiocarbon, 12*, 486-495, 1970.

Fergusson, G.J., Upper tropospheric carbon 14 levels during spring 1962, *J. Geophys. Res., 68*(13), 3933-3941, 1963.

Fortune, S.J., A sweepline algorithm for Voronoi diagrams, *Algorithmica, 2*, 153-174, 1987.

Godwin, H., and E.H. Willis, Cambridge University natural radiocarbon measurements, *Radiocarbon, 6*, 116-137, 1964.

Hagemann, F., and J. Gray Jr., Stratospheric carbon-14, carbon dioxide and tritium, *Science, 130*, 542-552, 1959.

Hagemann, F.T., J. Gray Jr., and L. Machta, Carbon-14 measurements in the atmosphere - 1953 to 1964, *HASL Rep. 159*, Health and Safety Lab., U.S. At. Energy Comm., New York, 1965. (Available as HASL 159/LL from Natl. Tech. Inf. Serv., Springfield, Va.)

Hagemann, F.T., J. Gray Jr., and L. Machta, Carbon-14 measurements in the atmosphere, *HASL Rep. 166*, Health and Safety Lab., U.S. At. Energy Comm., New York, 1966. (Available as HASL 166/LL from Natl. Tech. Inf. Serv., Springfield, Va.)

Hagemann, F.T., J. Gray Jr., and L. Machta, Carbon-14 measurements in the atmosphere, edited by E.P. Harvey Jr., and J. Rivera, *HASL Rep. 174*, pp. III-42 - III-70, Health and Safety Lab., U.S. At. Energy Comm., New York, 1967. (Available as HASL 174/LL from Natl. Tech. Inf. Serv., Springfield, Va.)

Hagemann, F.T., J. Gray Jr., and L. Machta, Carbon-14 measurements in the atmosphere, edited by E.P. Harvey Jr., and J. Rivera, *HASL Rep. 214*, pp. III-44 - III-80, Health and Safety Lab., U.S. At. Energy Comm., New York, 1969. (Available as HASL 214/LL from Natl. Tech. Inf. Serv., Springfield, Va.)

Hagemann, F.T., J. Gray Jr., and L. Machta, Carbon-14 measurements in the atmosphere, edited by E.P. Harvey Jr., *HASL Rep. 242*, pp. III-63 - III-75, Health and Safety Lab., U.S. At. Energy Comm., New York, 1971. (Available as HASL 242/LL from Natl. Tech. Inf. Serv., Springfield, Va.)

Hesshaimer, V., Tracing the global carbon cycle with bomb radiocarbon, Ph.D. thesis, Univ. of Heidelberg, Heidelberg, Germany, 1997.

Hesshaimer, V., M. Heimann, and I. Levin, Radiocarbon evidence for a smaller oceanic carbon dioxide sink than previously believed, *Nature, 370*, 201-203, 1994.

Jain, A.K., H.S. Kheshgi, and D.J. Wuebbles, Is there an imbalance in the global budget of bomb-produced radiocarbon?, *J. Geophys. Res., 102*(D1), 1327-1333, 1997.

Johnston, H.S., Evaluation of excess carbon 14 and strontium 90 data for suitability to test two-dimensional stratospheric models, *J. Geophy. Res., 94*(D15), 18,485-18,493, 1989.

Karlén, I., I.U. Olsson, P. Kallenberg, and S. Kilici, Absolute determination of the activity of two ^{14}C dating standards, *Ark. Geofys., 4*(22), 465-471, 1968.

Keeling, C.D., and T.P. Whorf, CO_2 observations at Mauna Loa, Hawaii, in *Trends 90*, edited by T.A. Boden, P. Kanciruk, and M.P. Farrell, pp. 8-9, Oak Ridge Natl. Lab., Oak Ridge, Tenn., 1990.

Kinnison, D.E., H.S. Johnston, and D.J. Wuebbles, Model study of atmospheric transport using carbon 14 and strontium 90 as inert tracers, *J. Geophys. Res., 99*(D10), 20,647-20,664, 1994.

Lassey, K.R., I.G. Enting, and C.M. Trudinger, The Earth's radiocarbon budget: A consistent model of the global carbon and radiocarbon cycles, *Tellus, 48B*, 487-501, 1996.

Leifer, R., and N. Chan, The Environmental Measurements Laboratory's stratospheric radionuclide (RANDAB) and trace gas (TRACDAB) databases, *CDIAC Commun. 24*, p. 14, Carbon Dioxide Inf. Anal. Cent., Oak Ridge, Tenn., 1998.

Levin, I., B. Kromer, H. Schoch-Fischer, M. Bruns, M. Münnich, D. Berdau, J.C. Vogel, and K.O. Münnich, 25 years of tropospheric ^{14}C observations in Central Europe, *Radiocarbon, 27*(1), 1-19, 1985.

Libby, W.F., E.C. Anderson, and J.R. Arnold, Age determination by radiocarbon content: World-wide assay of natural radiocarbon, *Science, 109*, 227-228, 1949.

Lingenfelter, R.E., Production of carbon 14 by cosmic-ray neutrons, *Rev. Geophys., 1*(1), 35-55, 1963.

Manning, M.R., D.C. Lowe, W.H. Melhuish, R.J. Sparks, G. Wallace, C.A.M. Brenninkmeijer, and R.C. McGill, The use of radiocarbon measurements in atmospheric studies, *Radiocarbon, 32*(1), 37-58, 1990.

Nydal, R., and K. Lövseth, Tracing bomb ^{14}C in the atmosphere 1962-1980, *J. Geophys. Res., 88*(C6), 3621-3642, 1983.

O'Brien, K., A. De La Zerda Lerner, M.A. Shea, and D.F. Smart, The production of cosmogenic isotopes in the Earth's atmosphere and their inventories, in *The Sun in Time*, edited by C.P. Sonnet, M.S. Giampapa, and M.S. Matthews, pp. 317-342, Univ. of Ariz. Press, Tucson, 1991.

Olsson, I.U. (Ed.), The use of oxalic acid as a standard, in *Radiocarbon Variations and Absolute Chronology, Nobel Symposium, 12th Proceedings*, p. 17, John Wiley, New York, 1970.

O'Rourke, J., *Computational Geometry in C*, Cambridge University Press, New York, 1994.

Rasch, P.J., X. Tie, B.A. Boville, and D.L. Williamson, A three-dimensional transport model for the middle atmosphere, *J. Geophys. Res., 99*(D1), 999-1017, 1994.

Rath, H.K., Simulation of the global ^{85}Kr and $^{14}CO_2$ distribution by means of a time dependent two-dimensional model of the atmosphere (in German), Ph.D. thesis, Univ. of Heidelberg, Heidelberg, Germany, 1988.

Shia, R.-L., M.K.W. Ko, M. Zou, and V.R. Kotamarthi, Cross-tropopause transport of excess ^{14}C in a two-dimensional model, *J. Geophys. Res., 98*(D10), 18,599-18,606, 1993.

Sowl, R.E., J. Gray Jr., T.E. Ashenfelter, and K. Telegadas, Carbon-14 measurements in the stratosphere from a balloon-borne molecular sieve sampler (1971-1973), edited by E.P. Hardy Jr., *HASL Rep. 284*, pp. I-64 - I-76, Health and Safety Lab., U.S. At. Energy Comm., New York, 1974. (Available as HASL 284 and APP/LL from Natl. Tech. Inf. Serv., Springfield, Va.)

Sowl, R.E., J. Gray Jr., T.E. Ashenfelter, and K. Telegadas, Carbon-14 measurements in the stratosphere from a balloon-borne molecular sieve sampler (1973-1974), edited by E.P. Hardy Jr., *HASL Rep. 294*, pp. I-20 - I-43, Health and Safety Lab., Energy

Res. and Development Admin., 1975. (Available as HASL 294/LL from Natl. Tech. Inf. Serv., Springfield, Va.)

Stuiver, M., and H.A. Polach, Discussion: Reporting of ^{14}C data, *Radiocarbon*, *19*(3), 355-363, 1977.

Tans, P., A compilation of bomb ^{14}C data for use in global carbon model calculations, in *Carbon Cycle Modelling (SCOPE 16)*, edited by B. Bolin, pp. 131-157, John Wiley, New York, 1981.

Telegadas, K., The seasonal atmospheric distribution and inventories of excess carbon-14 from March 1955 to July 1969, edited by E.P. Hardy Jr., *HASL Rep. 243*, pp. I-2 - I-87, Health and Safety Lab., U.S. At. Energy Comm., New York, 1971. (Available as HASL 243/LL from Natl. Tech. Inf. Serv., Springfield, Va.)

Telegadas, K., J. Gray Jr., R.E. Sowl, and T.E. Ashenfelter, Carbon-14 measurements in the stratosphere from a balloon-borne molecular sieve sampler, edited by E.P. Hardy Jr., *HASL Rep. 246*, pp. I-69 - I-106, Health and Safety Lab., U.S. At. Energy Comm., New York, 1972. (Available as HASL 246/LL from Natl. Tech. Inf. Serv., Springfield, Va.)

Trenberth, K.E., and C.J. Guillemot, The total mass of the atmosphere, *J. Geophys. Res.*, *99*(D11), 23,079-23,088, 1994.

Walton, A., M. Ergin, and D.D. Harkness, Carbon-14 concentrations in the atmosphere and carbon dioxide exchange rates, *J. Geophys. Res.*, *75*(15), 3089-3098, 1970.

Watson, D.F., *Contouring: A Guide to the Analysis and Display of Spatial Data*, Pergamon, Tarrytown, N.Y., 1994.

Yang, T.Y., *Finite Element Structural Analysis*, Prentice-Hall, Englewood Cliffs, N.J., 1986.

Yang, X., R. North, and C. Romney, PIDC Nuclear explosion database (revision 2), *Tech. Rep. CMR-99/16*, Cent. for Monit. Res., Airlington, Va., 1999.

V. Hesshaimer and I. Levin (corresponding author), Institut für Umweltphysik, University of Heidelberg, Im Neuenheimer Feld 229, Heidelberg, D-69120, Germany. (Ingeborg.Levin@iup.uni-heidelberg.de)

(Received August 30, 1999; revised November 5, 1999;
accepted November 12, 1999.)